Supplementary Material

An ultrasound assisted synthesis of spirooxindolo-1,2,4-oxadiazoles *via* [3+2] cycloaddition reaction and their anti-cancer activity

Madhu Kanchrana,[a] Bhargava Sai Allaka,[a] Gamidi Rama Krishna,[b] and Srinivas Basavoju [a,*]

[a]Department of Chemistry, National Institute of Technology Warangal, Hanamkonda-506 004, Telangana, India
[b]Organic Chemistry Division, CSIR-National Chemical Laboratory, Dr. Homi Bhabha Road, Pune, Maharashtra 411 008, India
Email: basavojusrinivas@nitw.ac.in

Table of Contents

1. 1H NMR spectrum of the compound 2

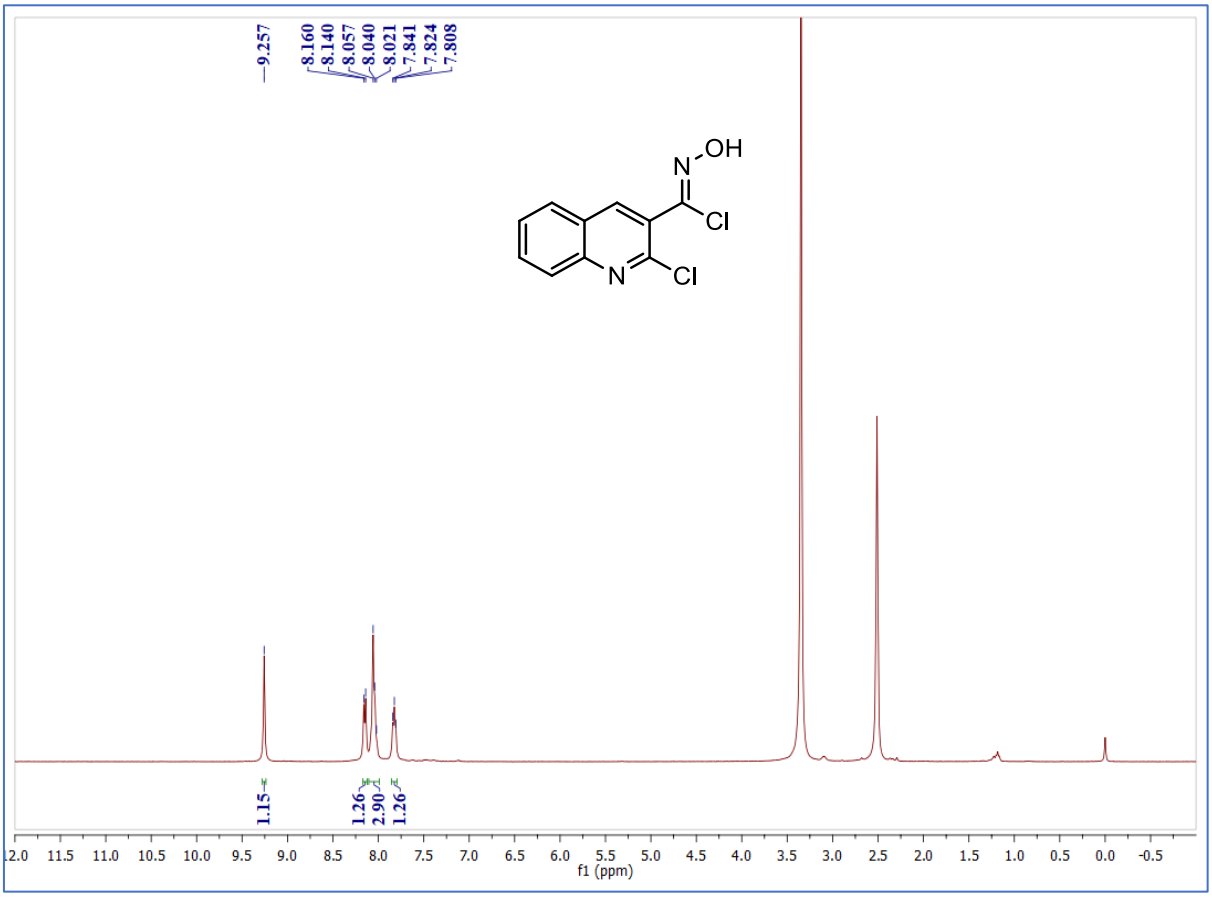

^{1}H NMR spectrum of the compound **2**

2. NMR, Mass, FTIR spectra of Compounds (3a-r)

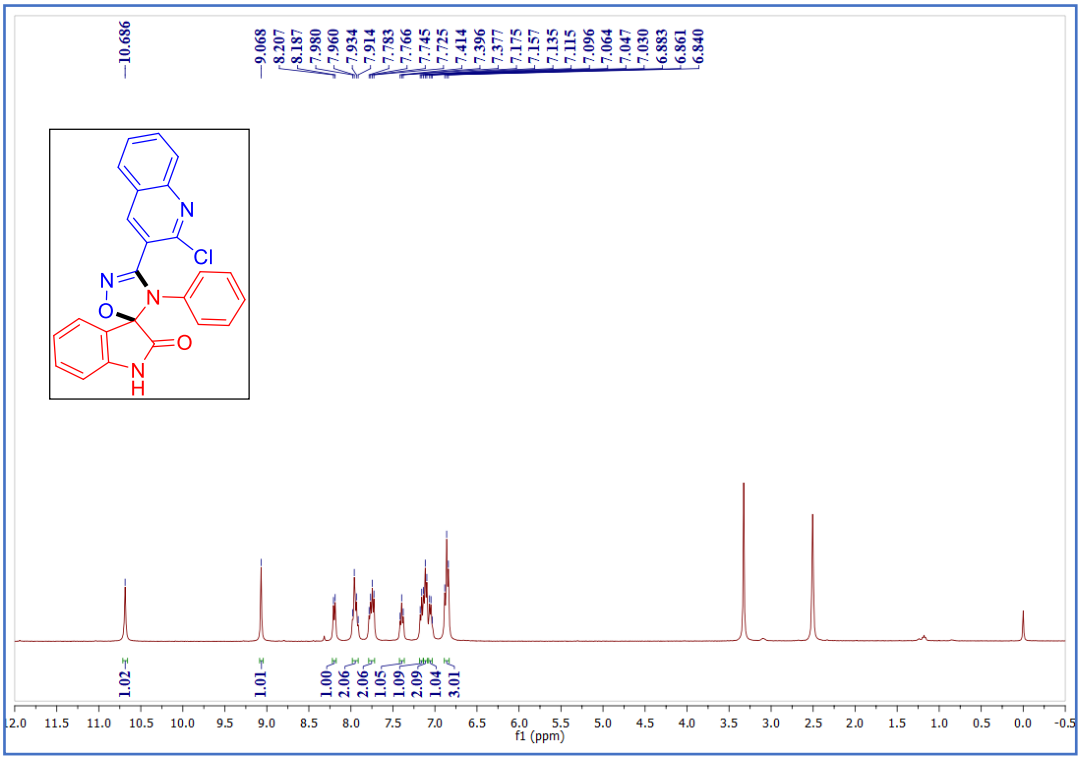

^{1}H NMR spectrum of the compound **3a**

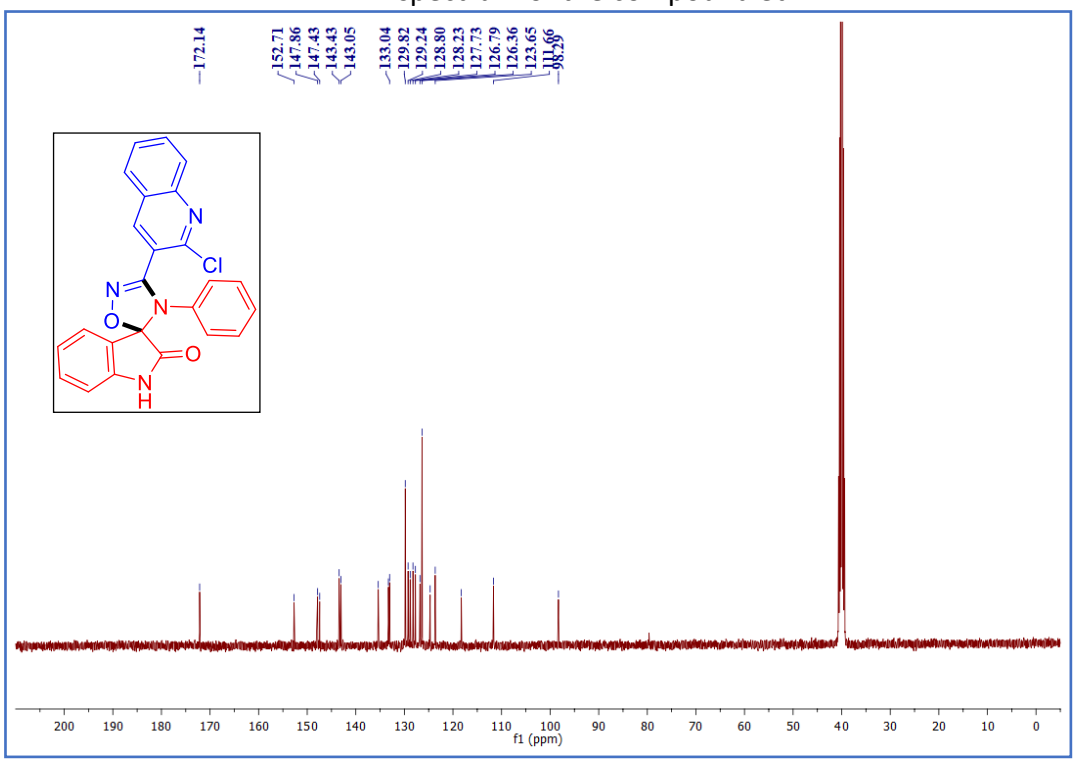

^{13}C NMR spectrum of the compound **3a**

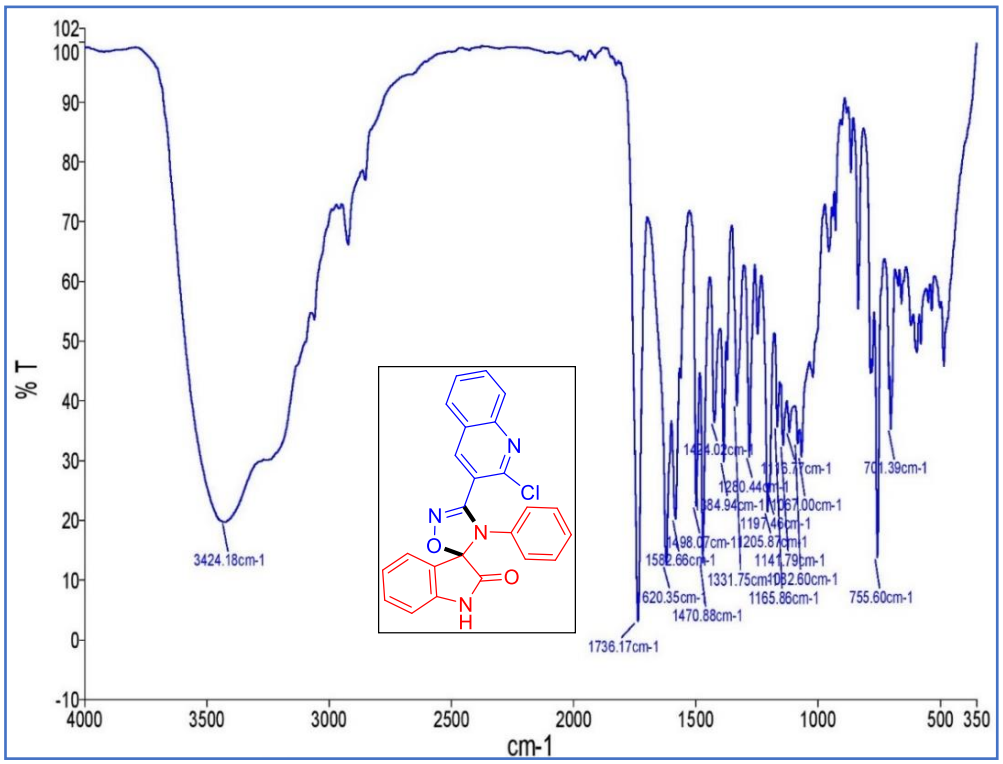

IR spectrum of the compound **3a**

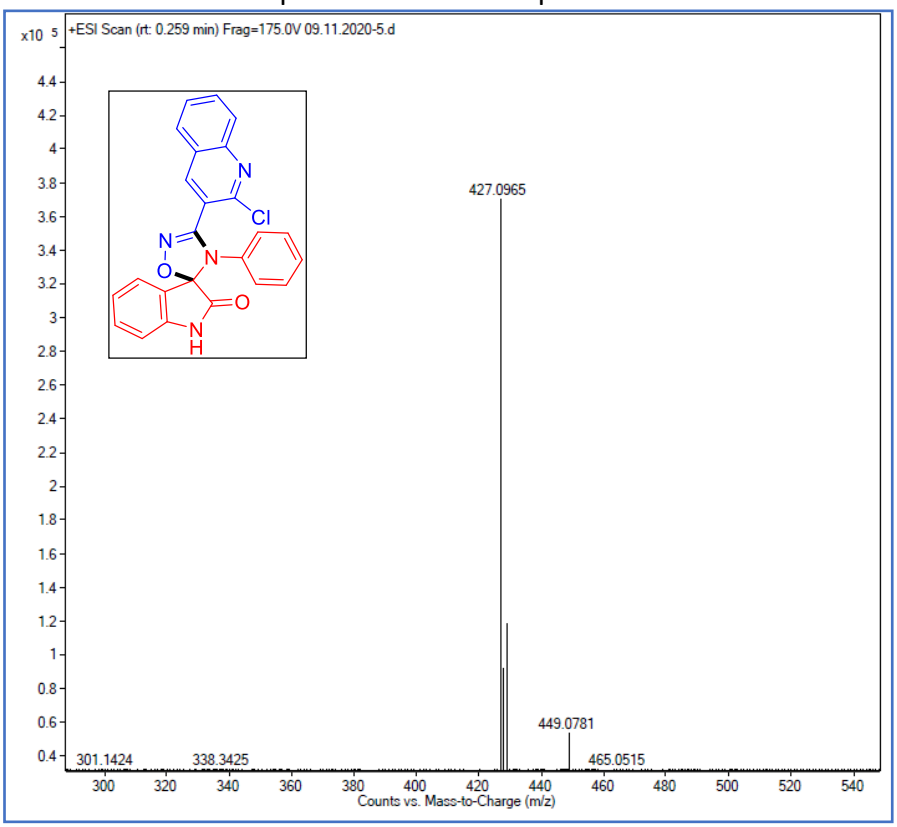

Mass spectrum of the compound **3a**

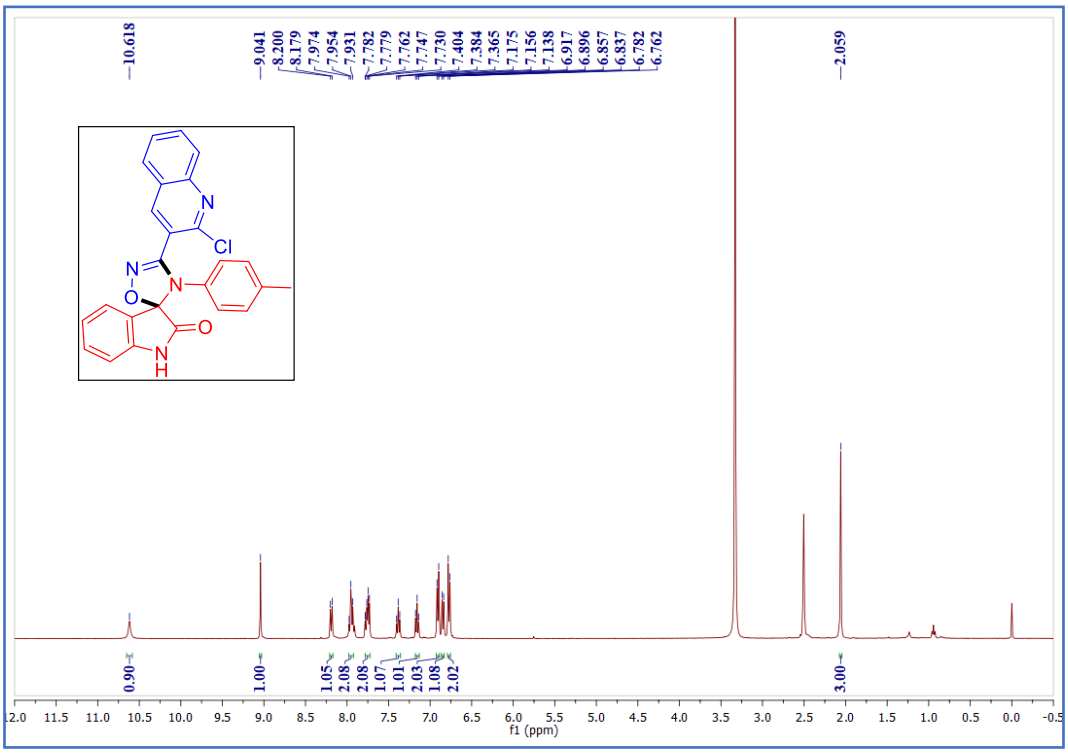

^{1}H NMR spectrum of the compound **3b**

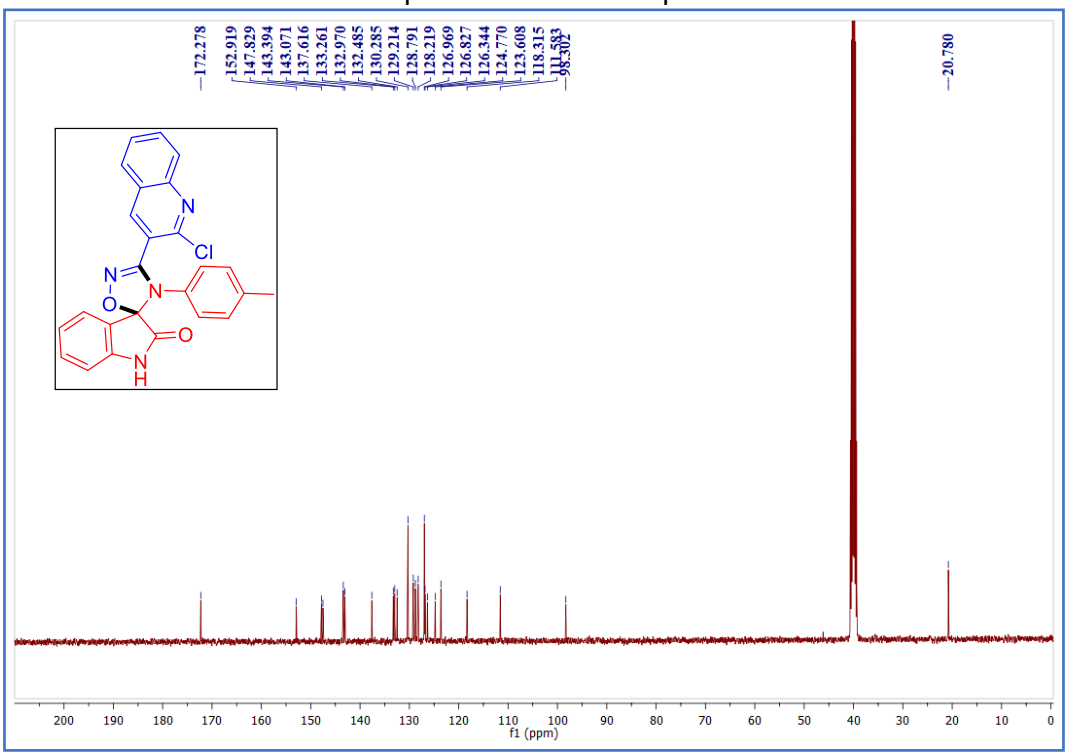

^{13}C NMR spectrum of the compound **3b**

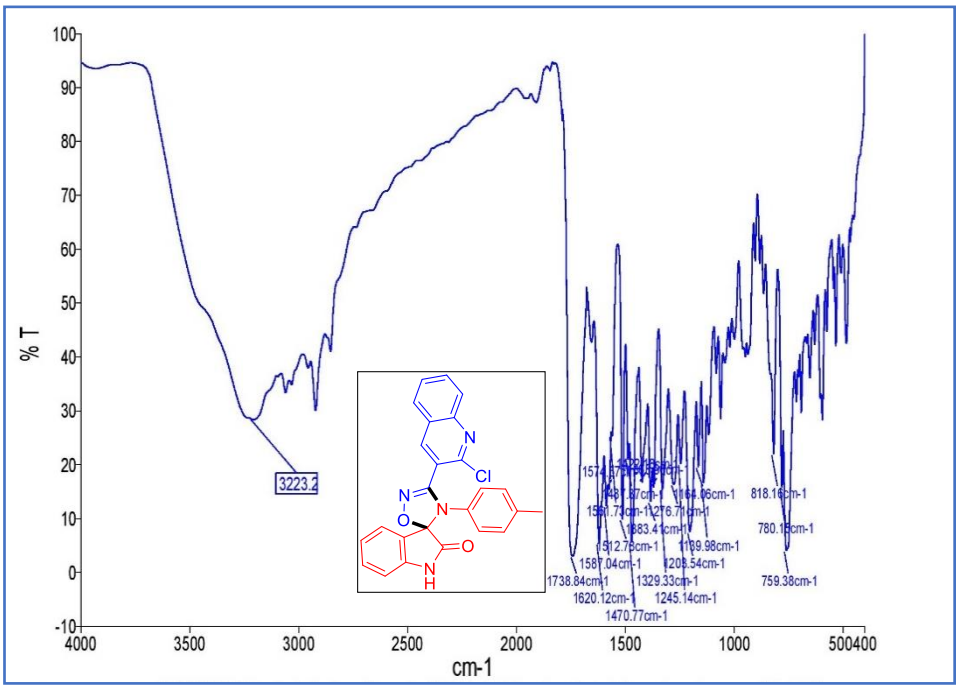

IR spectrum of the compound **3b**

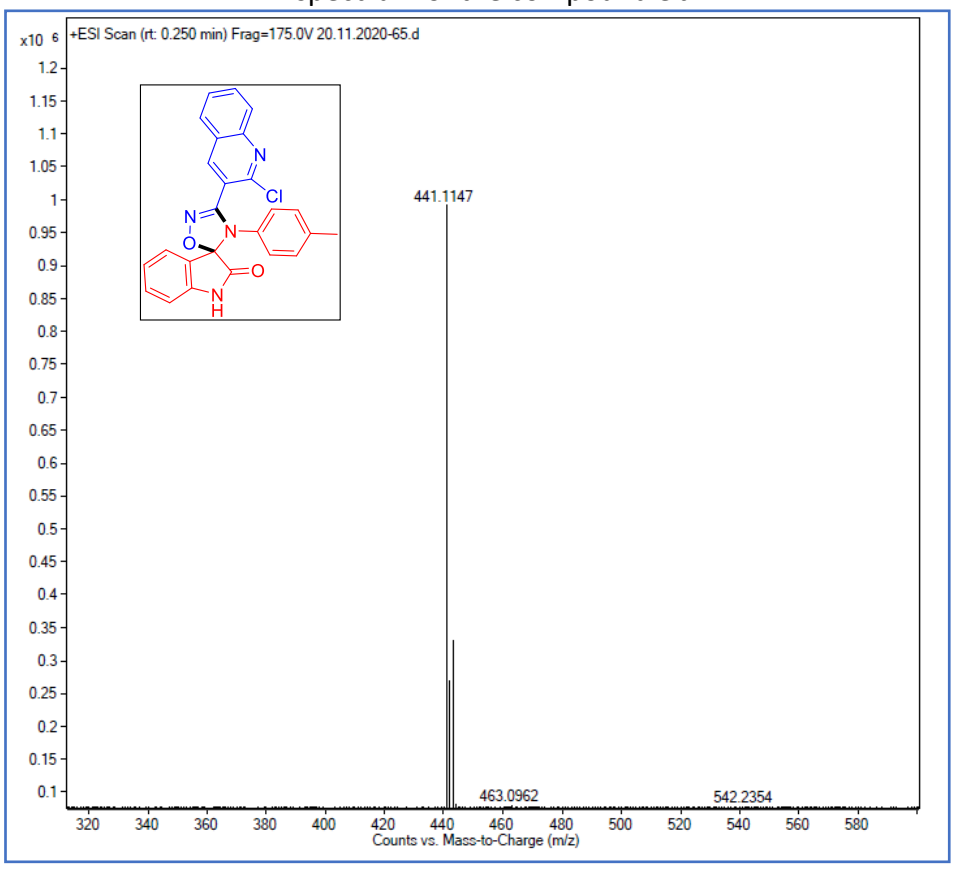

Mass spectrum of the compound **3b**

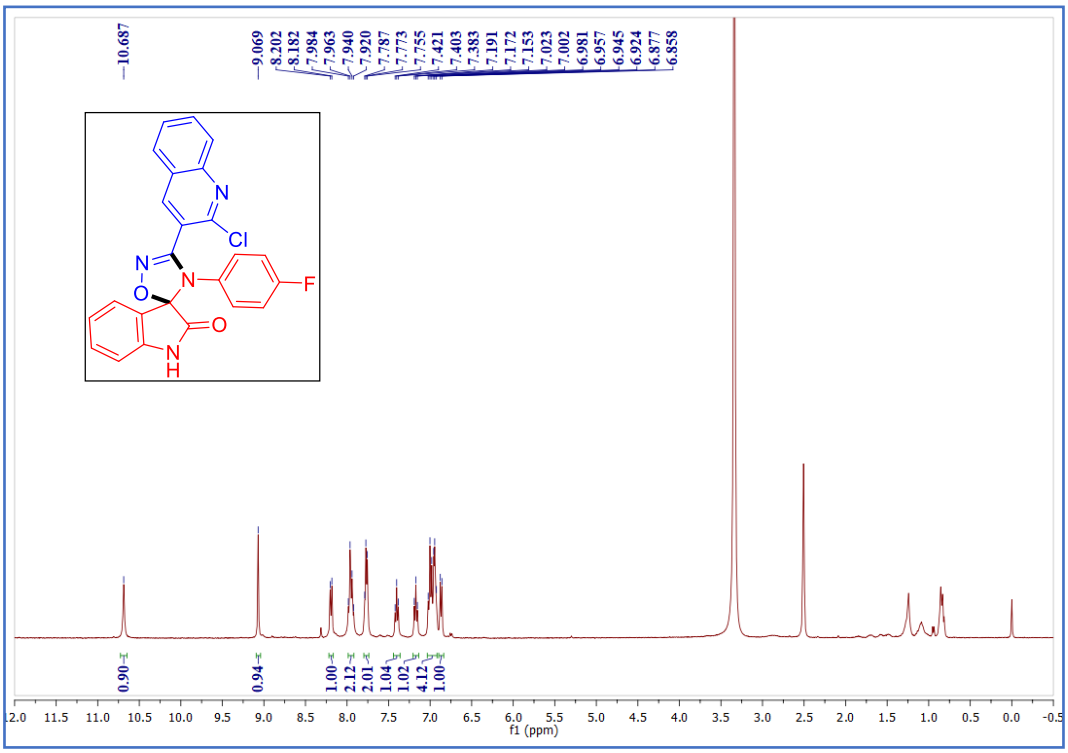

^{1}H NMR spectrum of the compound **3c**

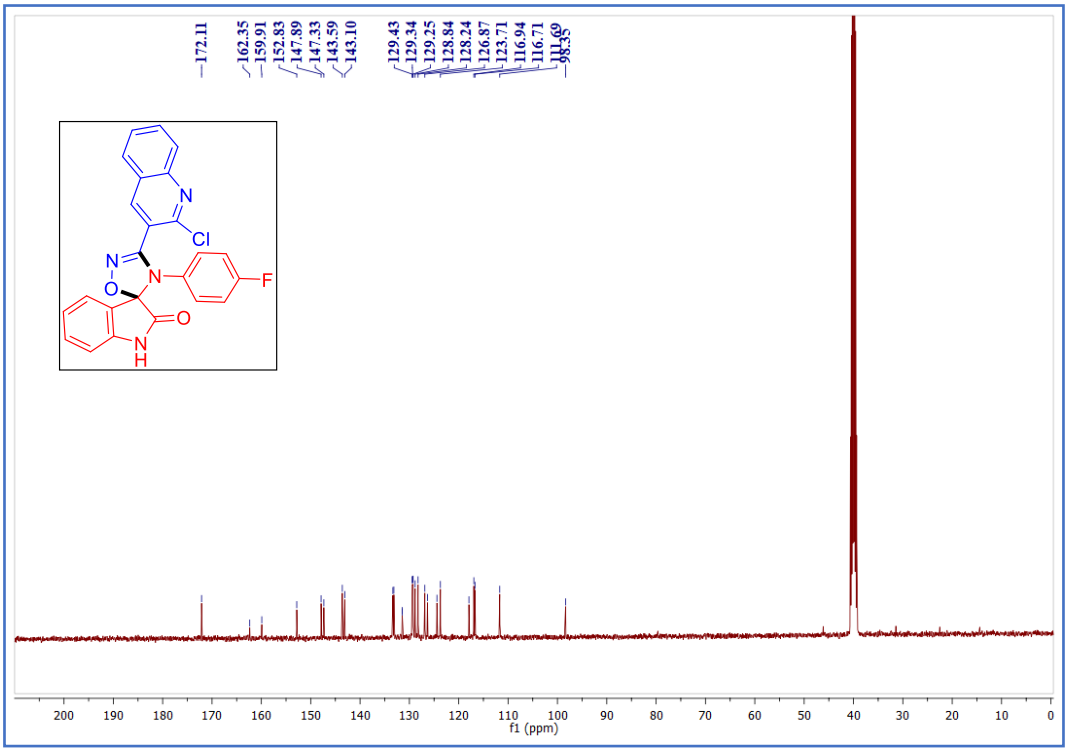

^{13}C NMR spectrum of the compound **3c**

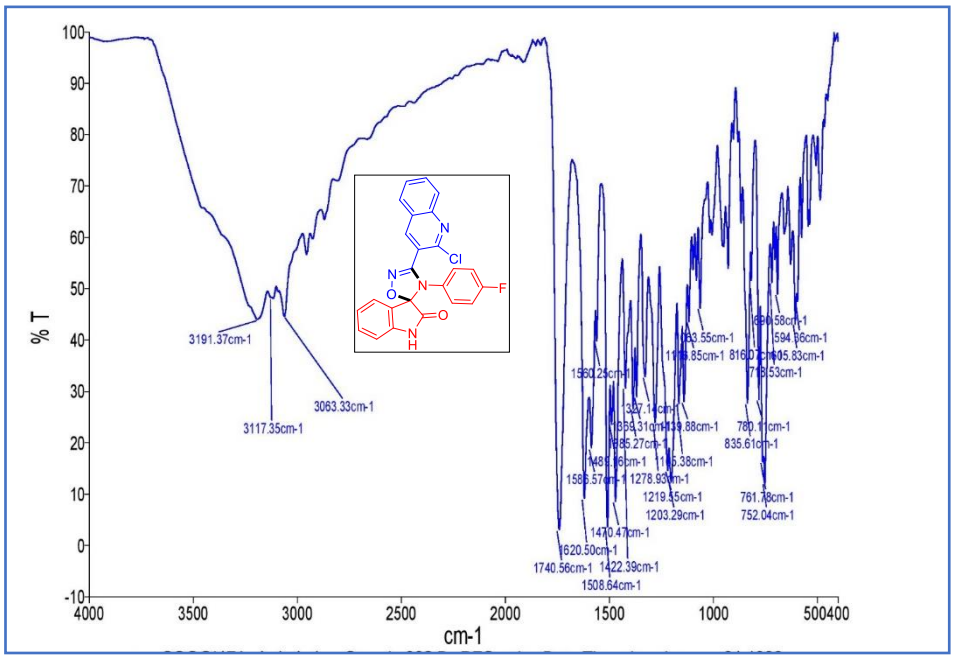

IR spectrum of the compound **3c**

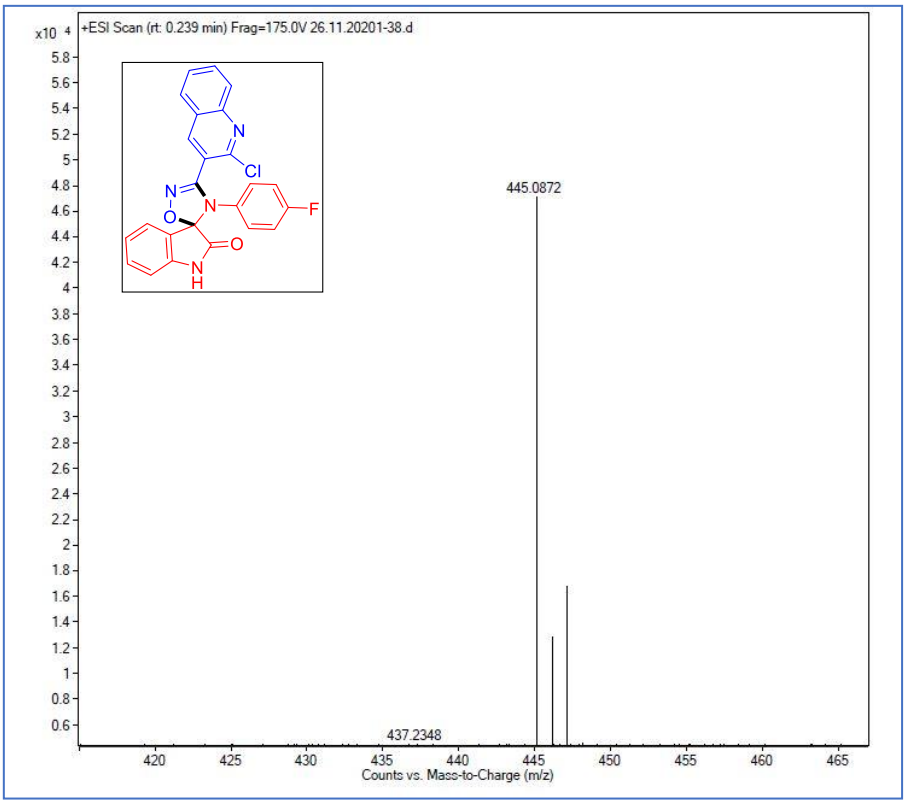

Mass spectrum of the compound **3c**

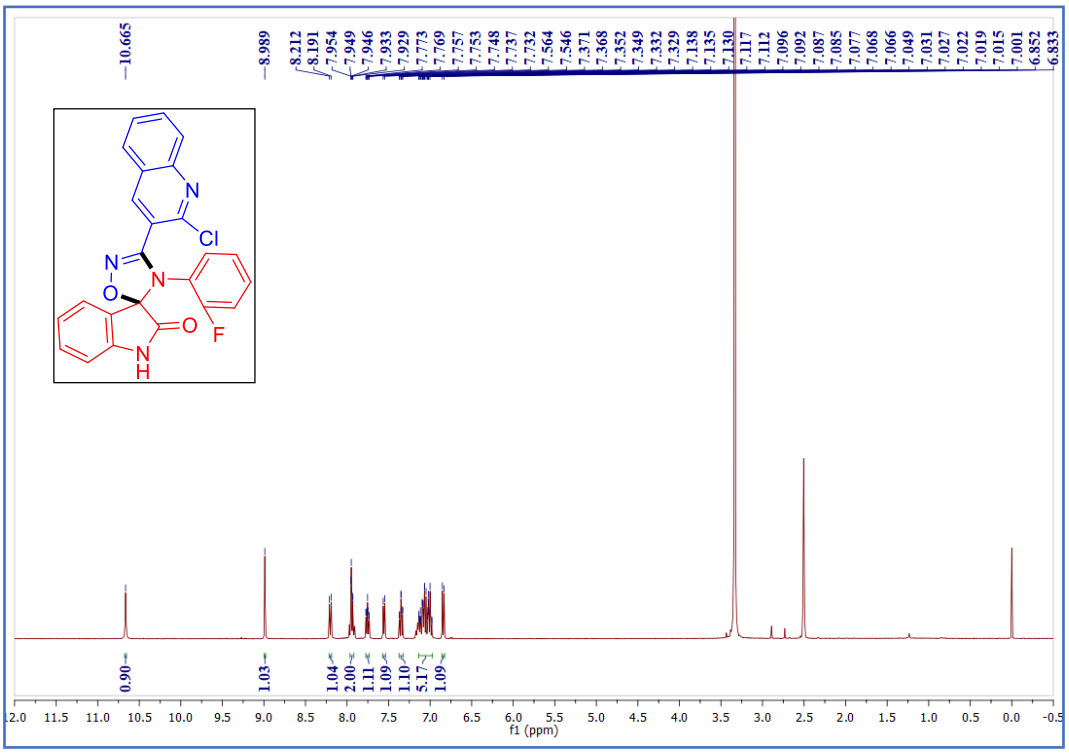

^{1}H NMR spectrum of the compound **3d**

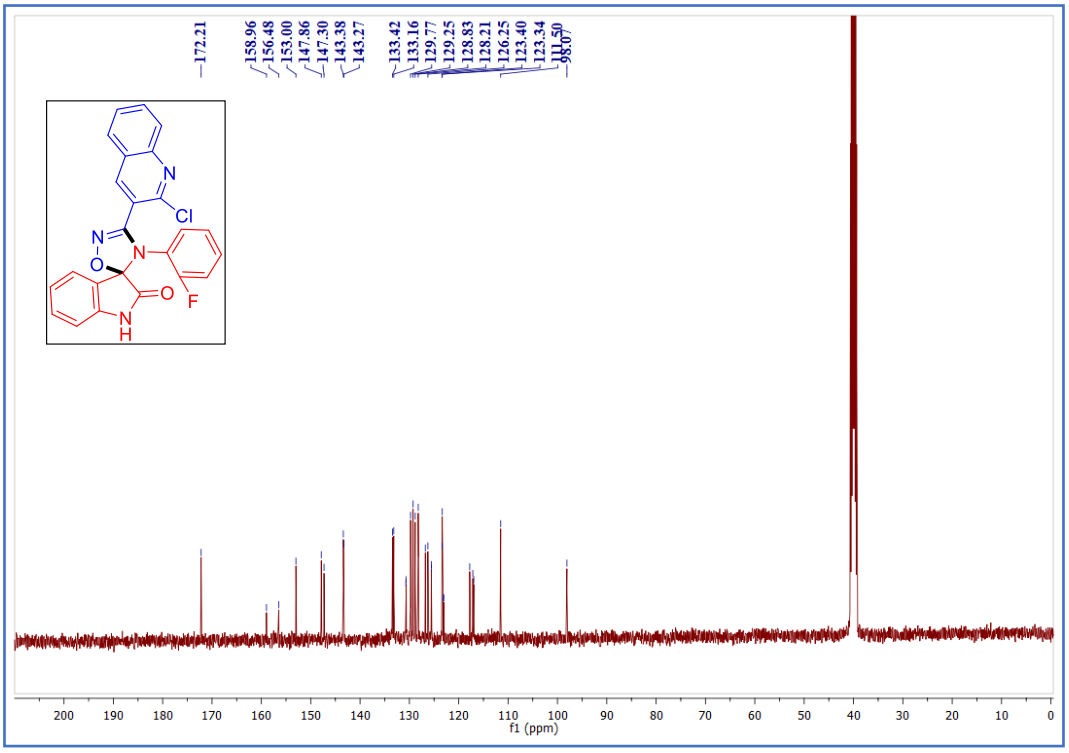

^{13}C NMR spectrum of the compound **3d**

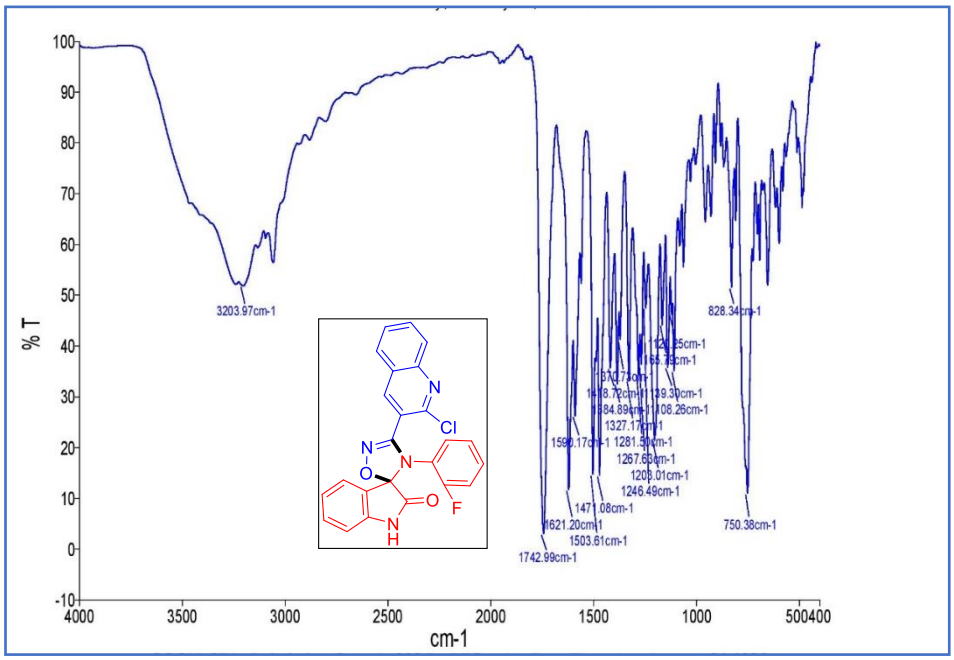

IR spectrum of the compound **3d**

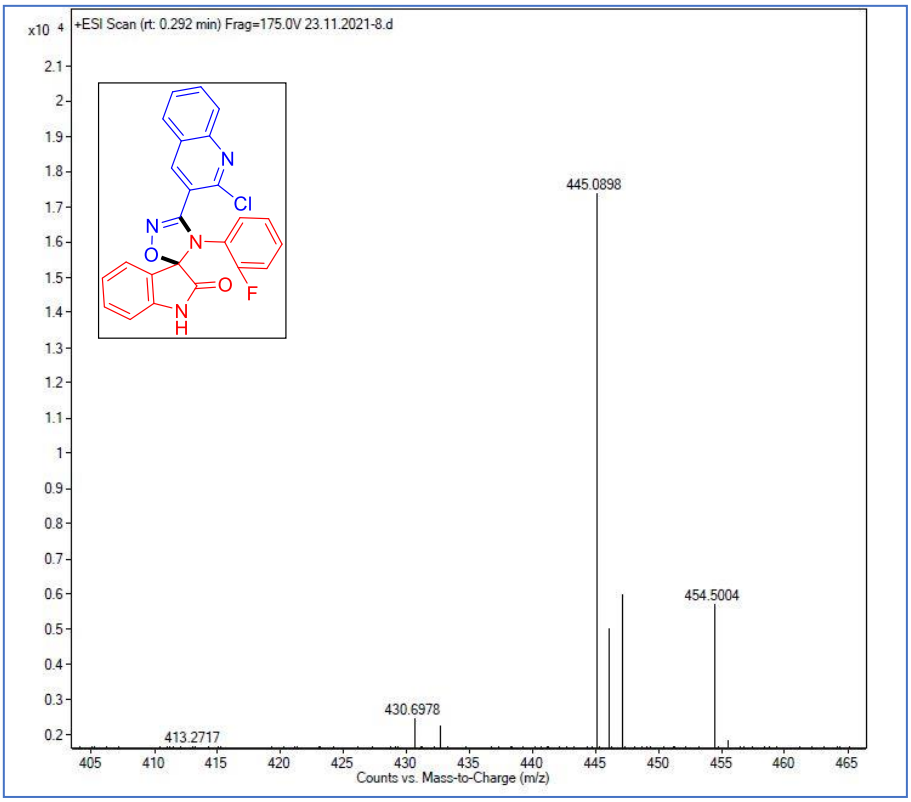

Mass spectrum of the compound **3d**

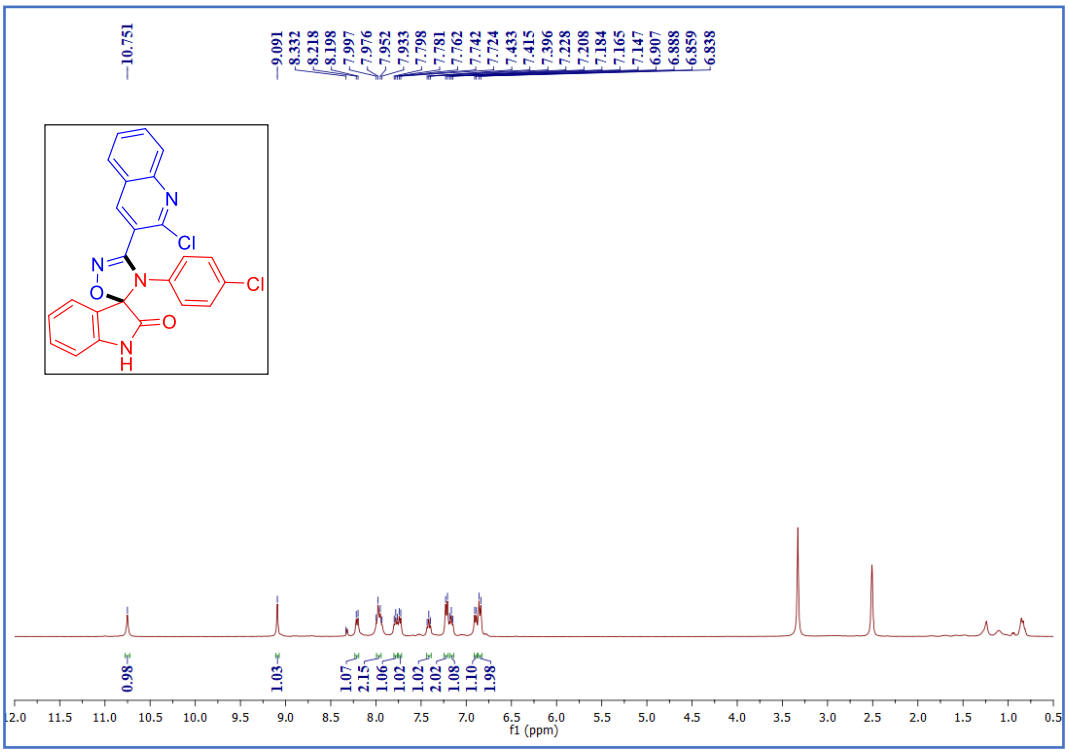

^{1}H NMR spectrum of the compound **3e**

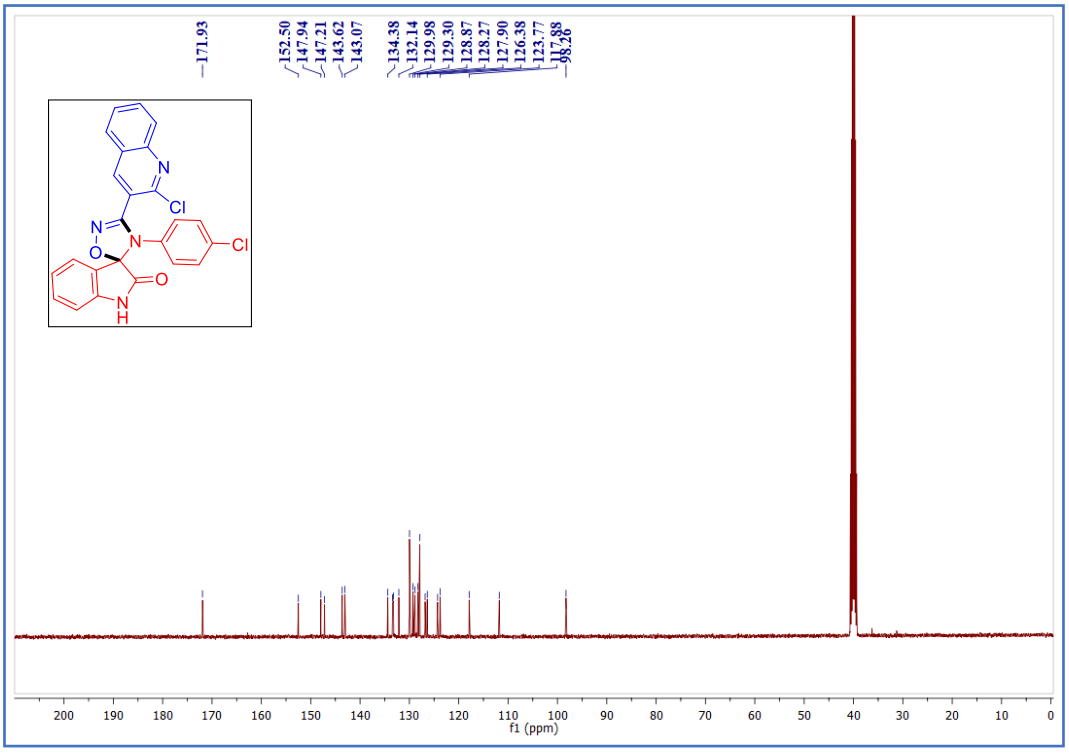

^{13}C NMR spectrum of the compound **3e**

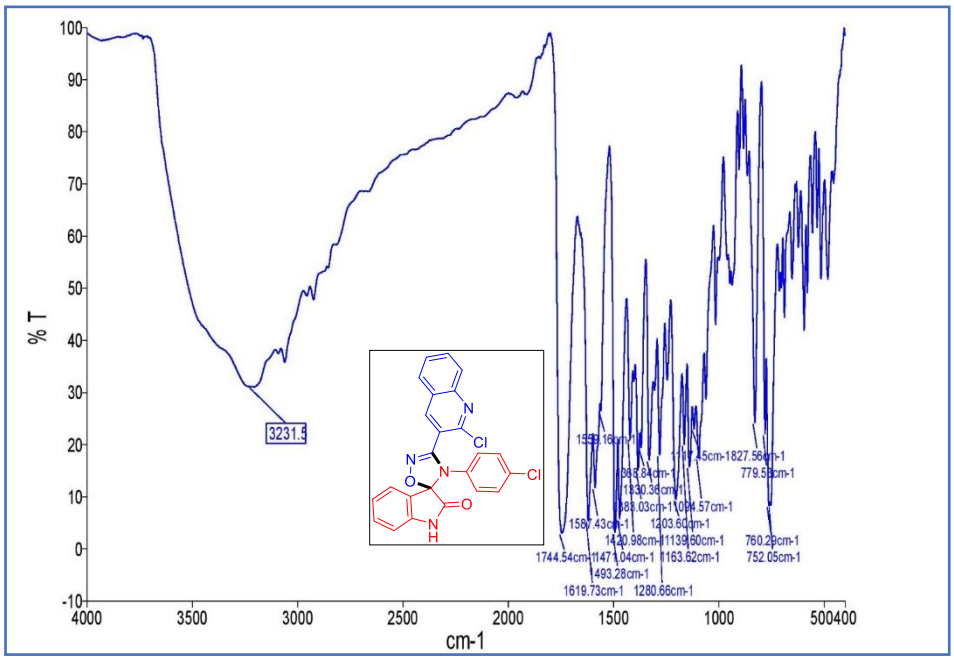

IR spectrum of the compound **3e**

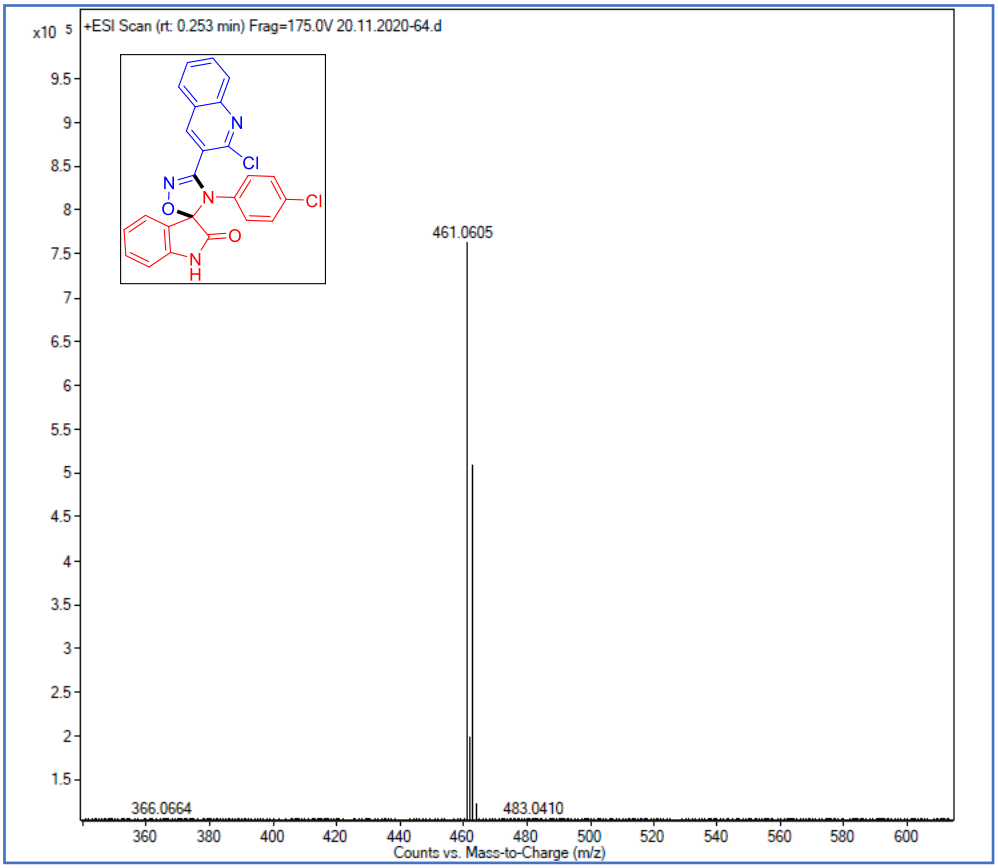

Mass spectrum of the compound **3e**

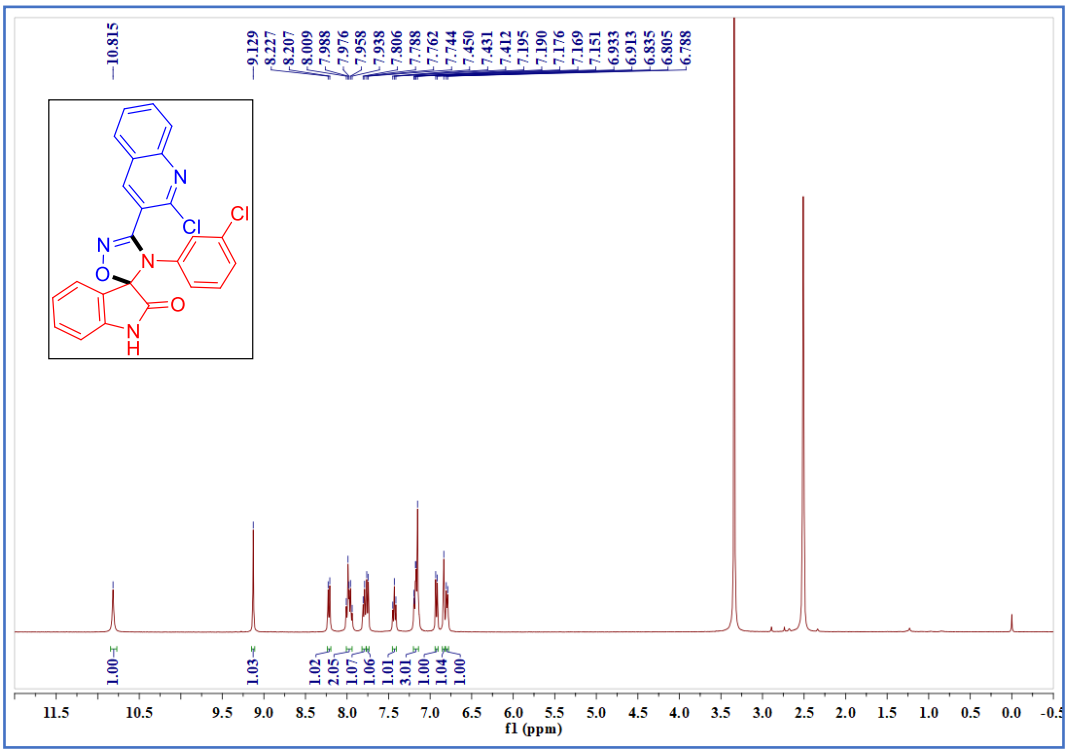

^{1}H NMR spectrum of the compound **3f**

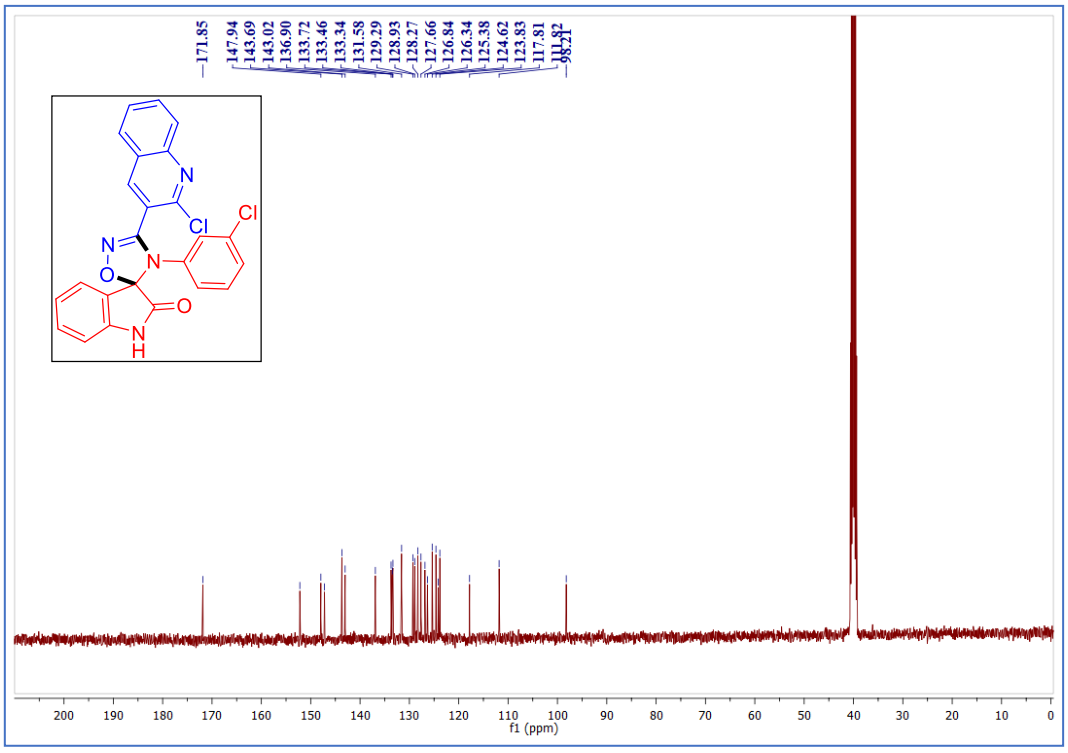

^{13}C NMR spectrum of the compound **3f**

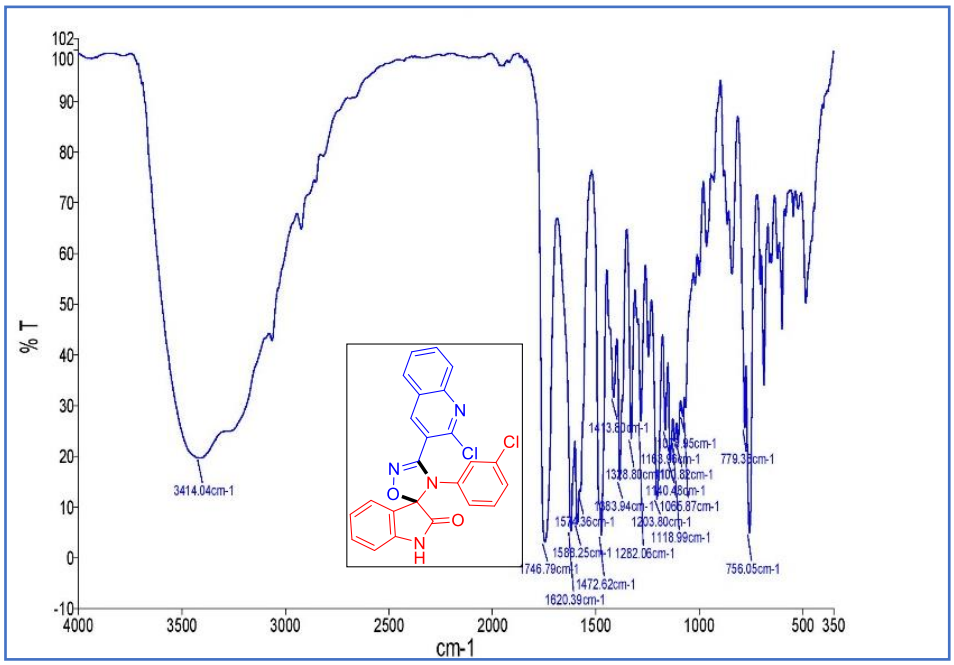

IR spectrum of the compound **3f**

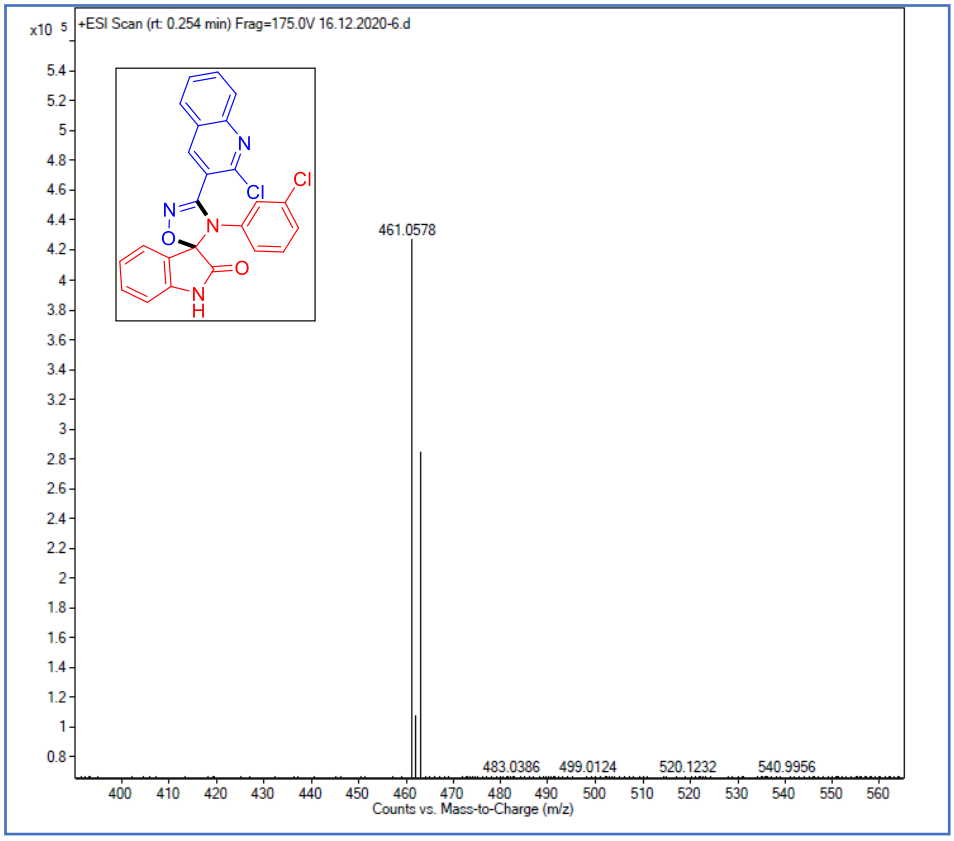

Mass spectrum of the compound **3f**

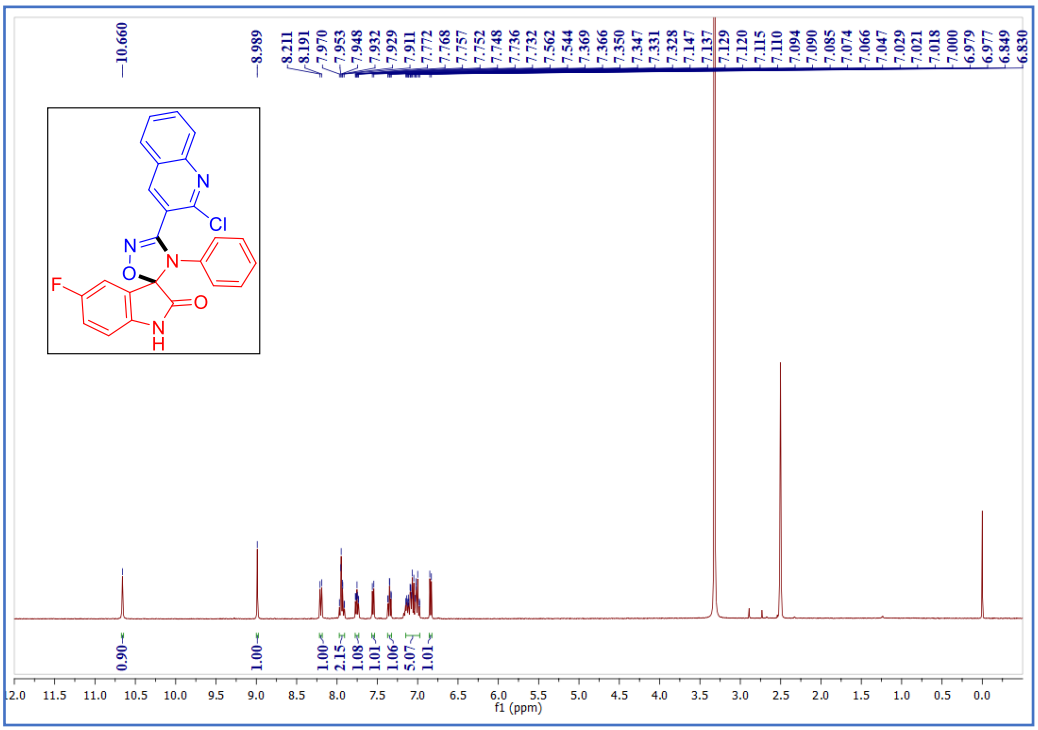

^{1}H NMR spectrum of the compound **3g**

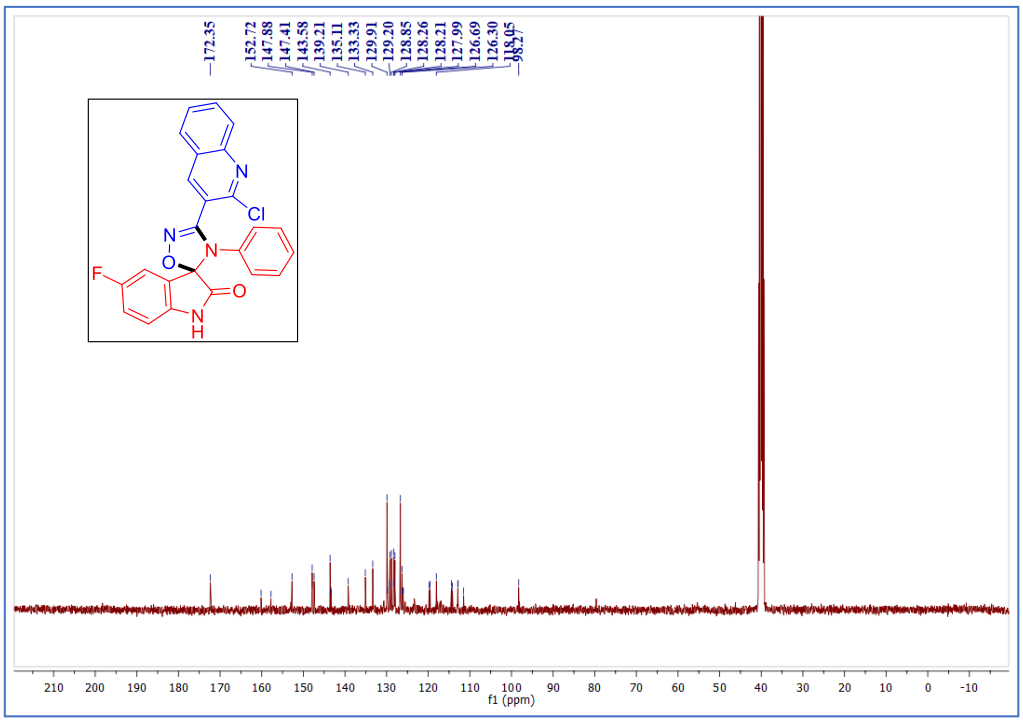

^{13}C NMR spectrum of the compound **3g**

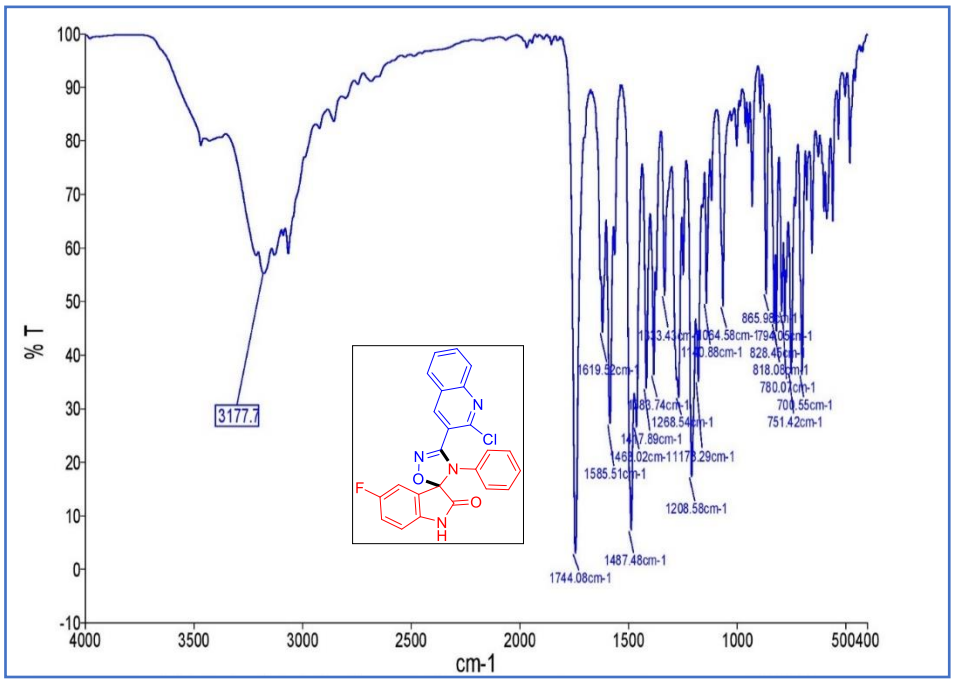

IR spectrum of the compound **3g**

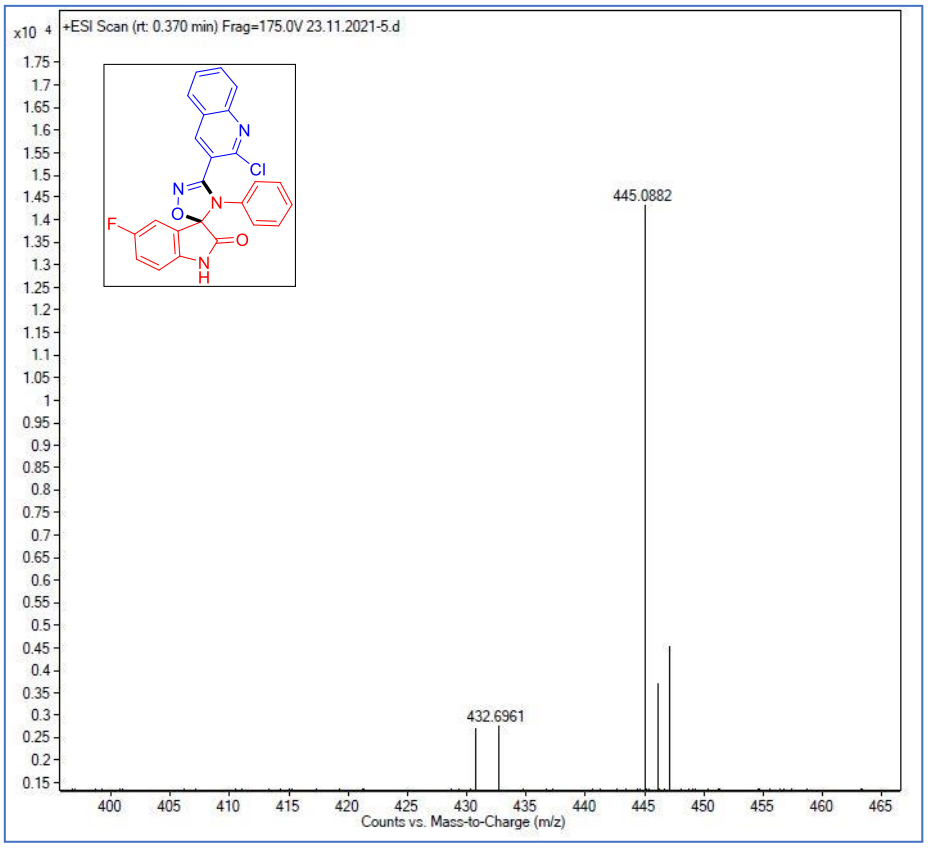

Mass spectrum of the compound **3g**

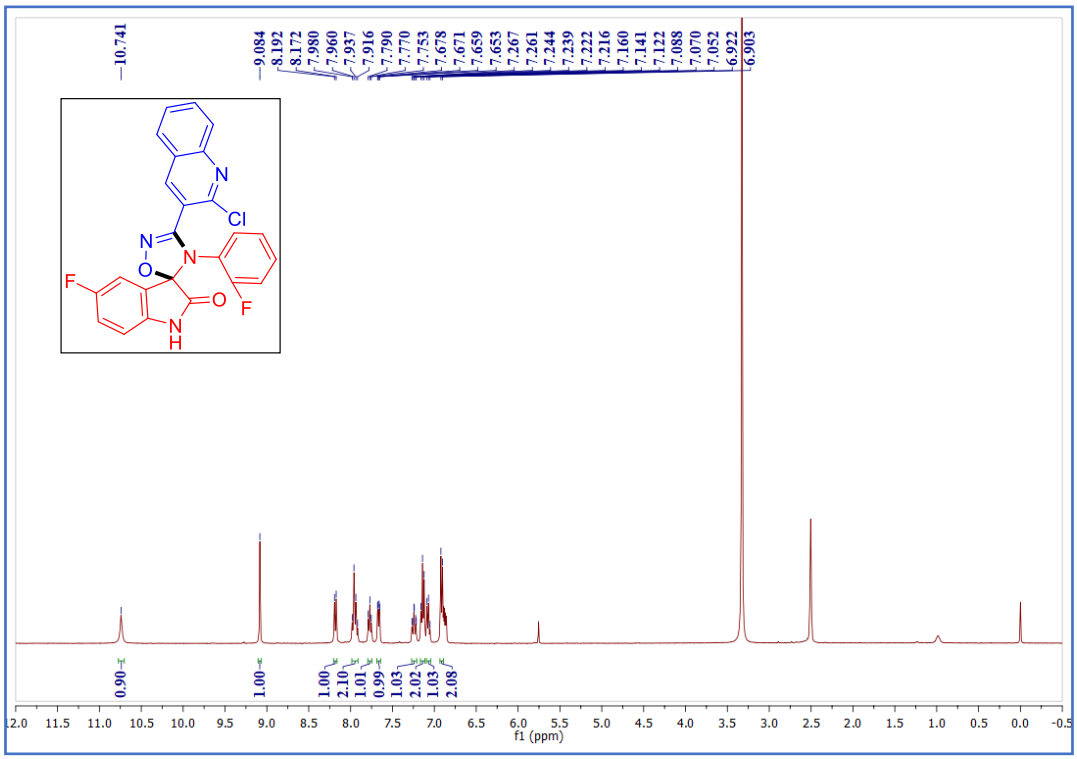

^{1}H NMR spectrum of the compound **3h**

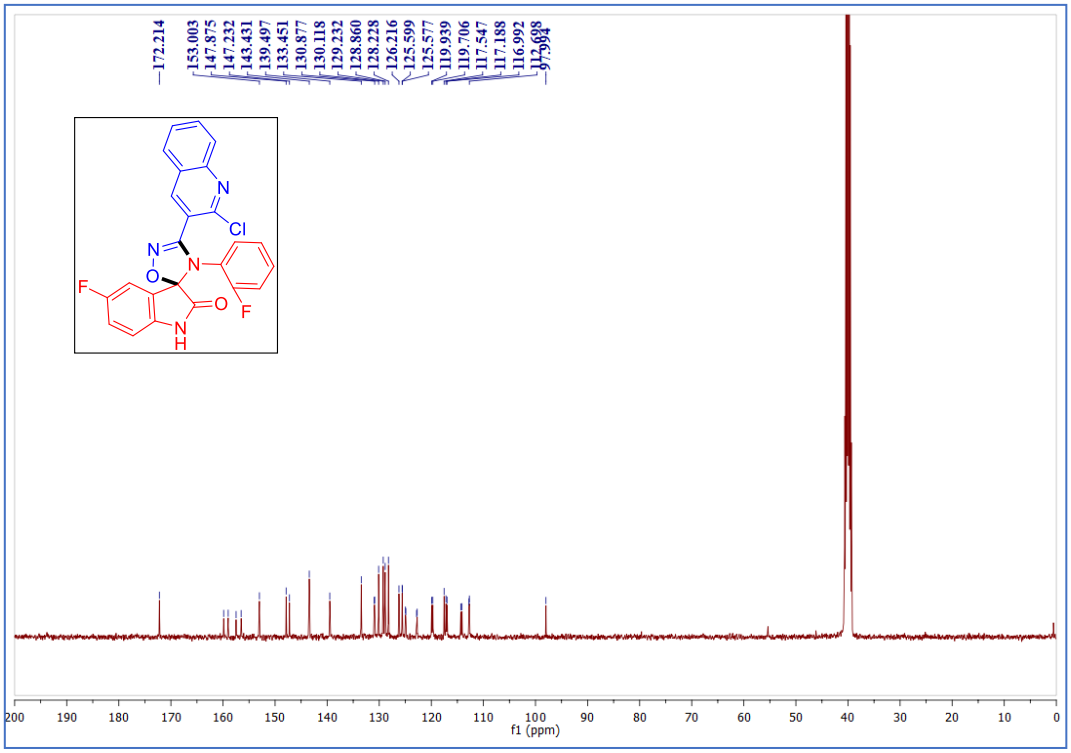

^{13}C NMR spectrum of the compound **3h**

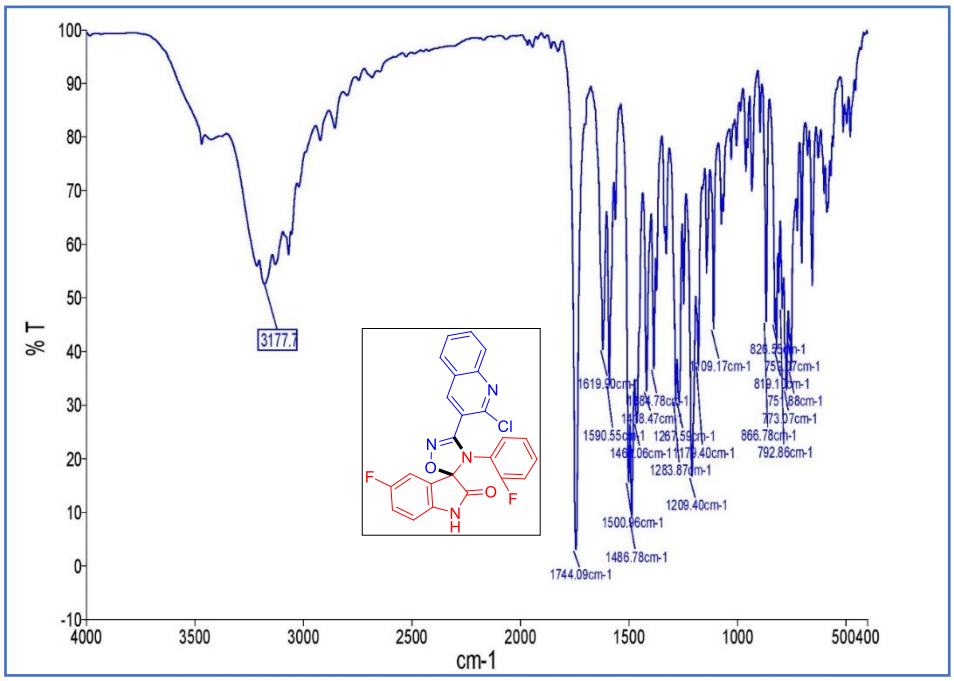

IR spectrum of the compound **3h**

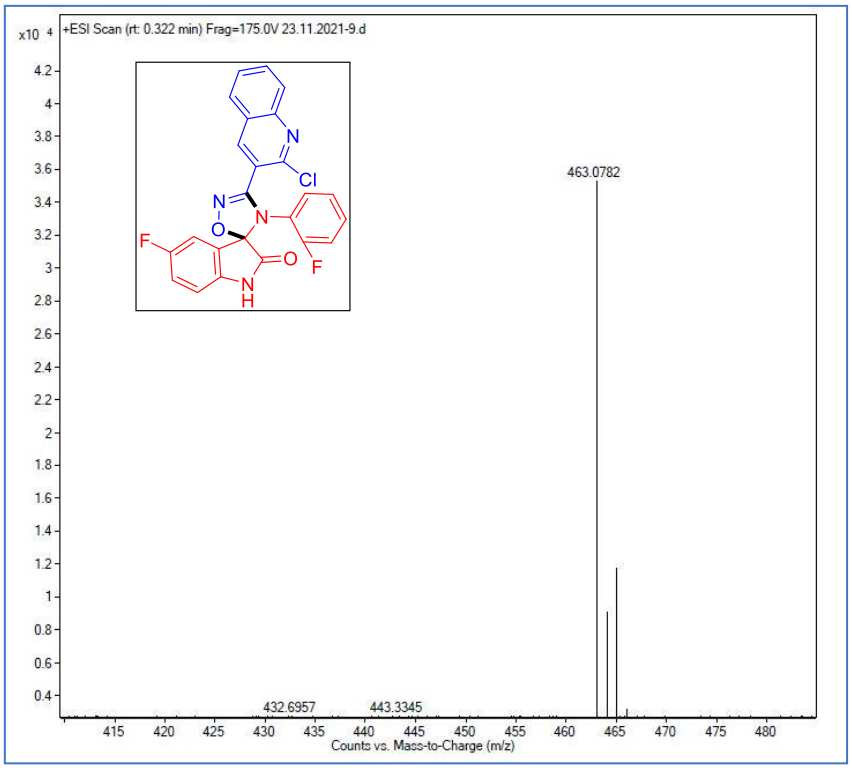

Mass spectrum of the compound **3h**

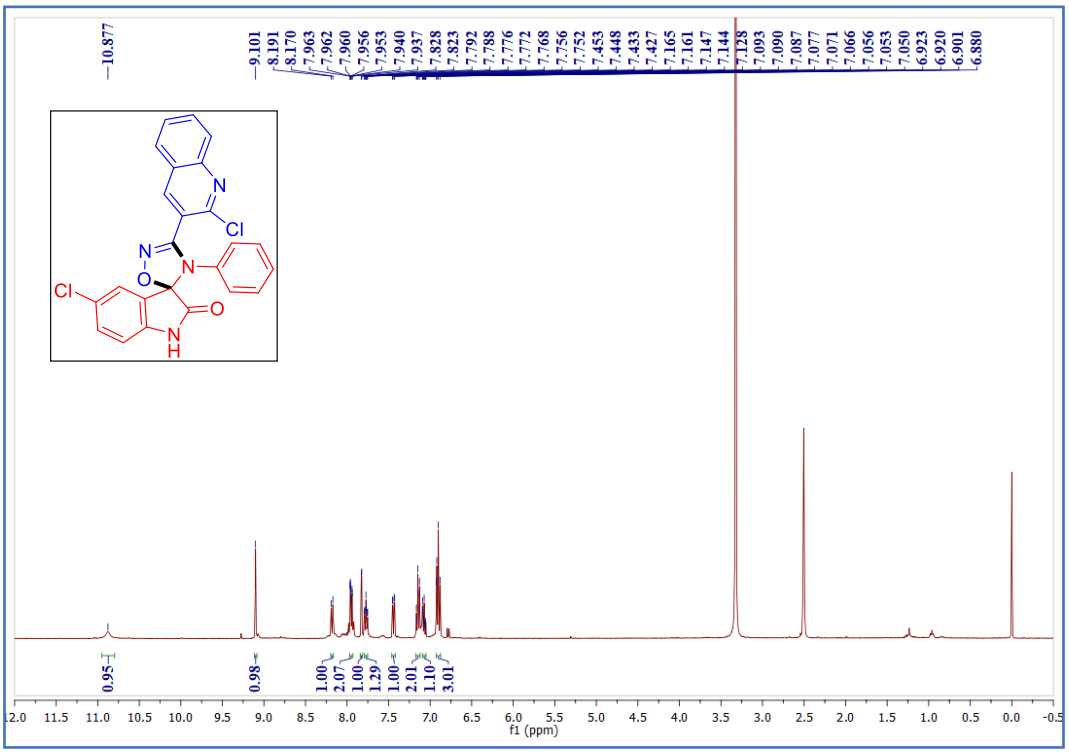

^{1}H NMR spectrum of the compound **3i**

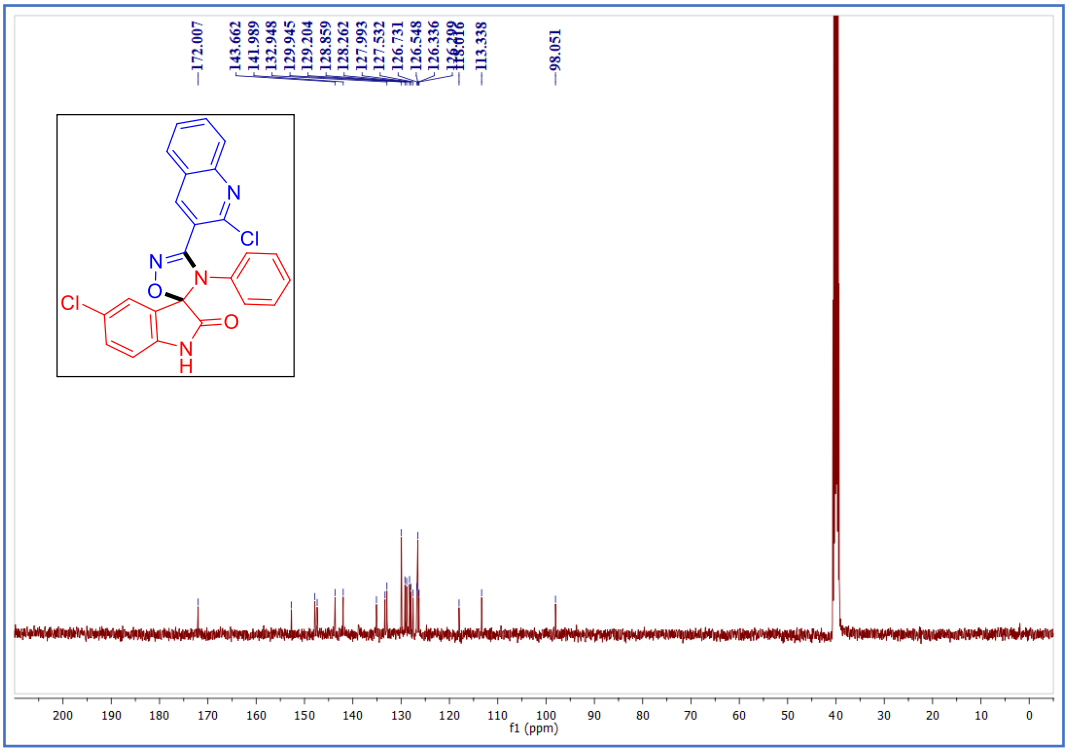

^{13}C NMR spectrum of the compound **3i**

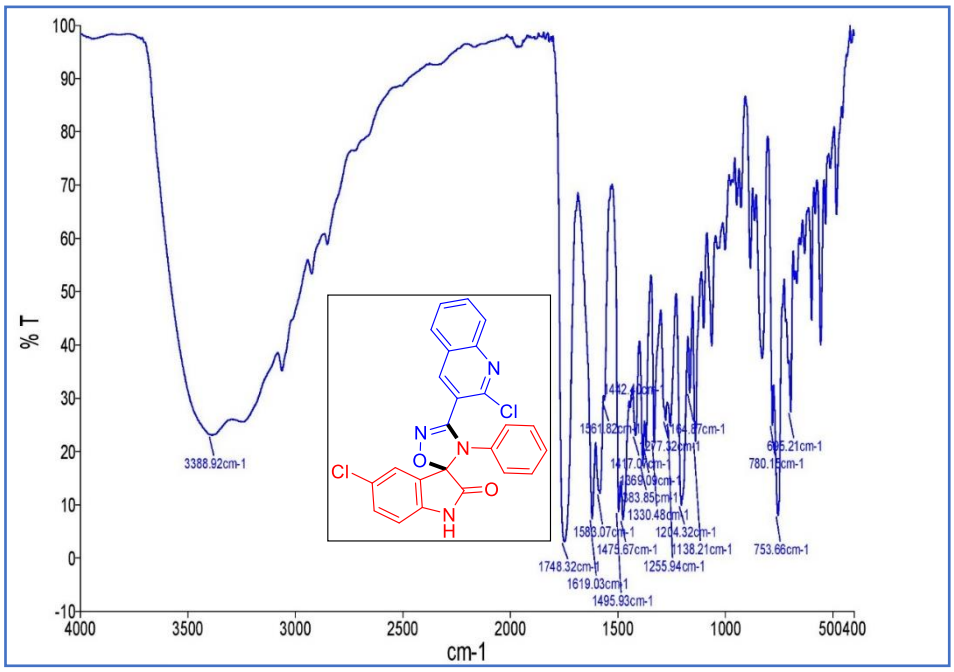

IR spectrum of the compound **3i**

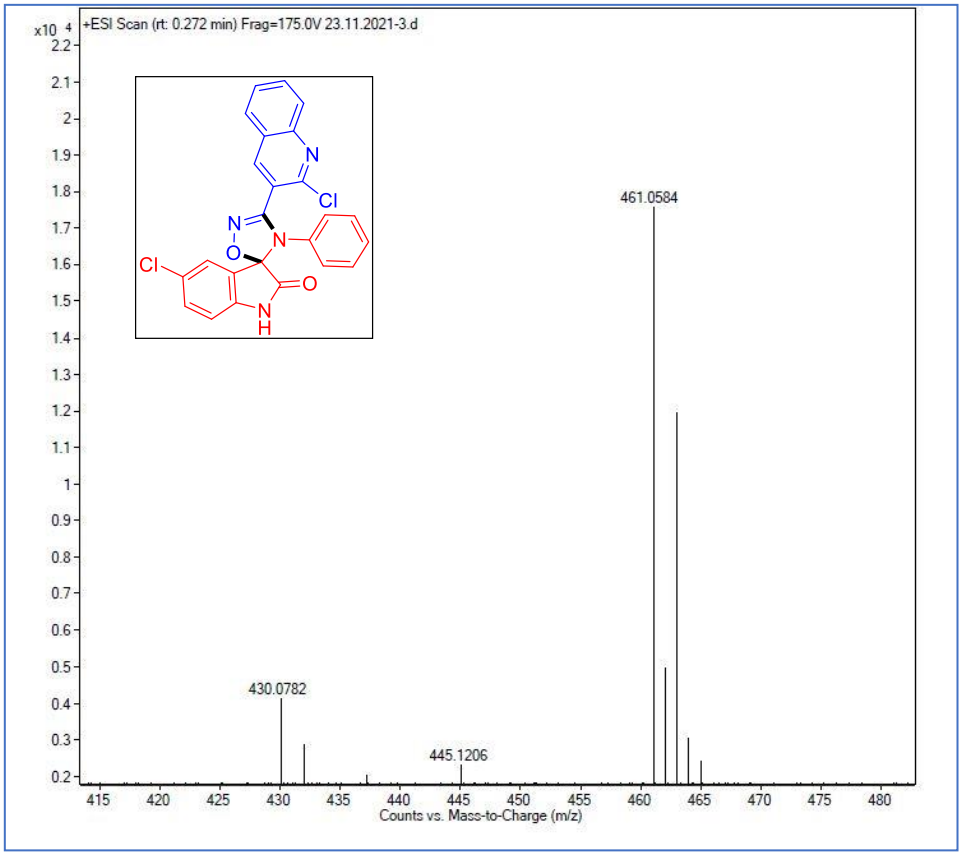

Mass spectrum of the compound **3i**

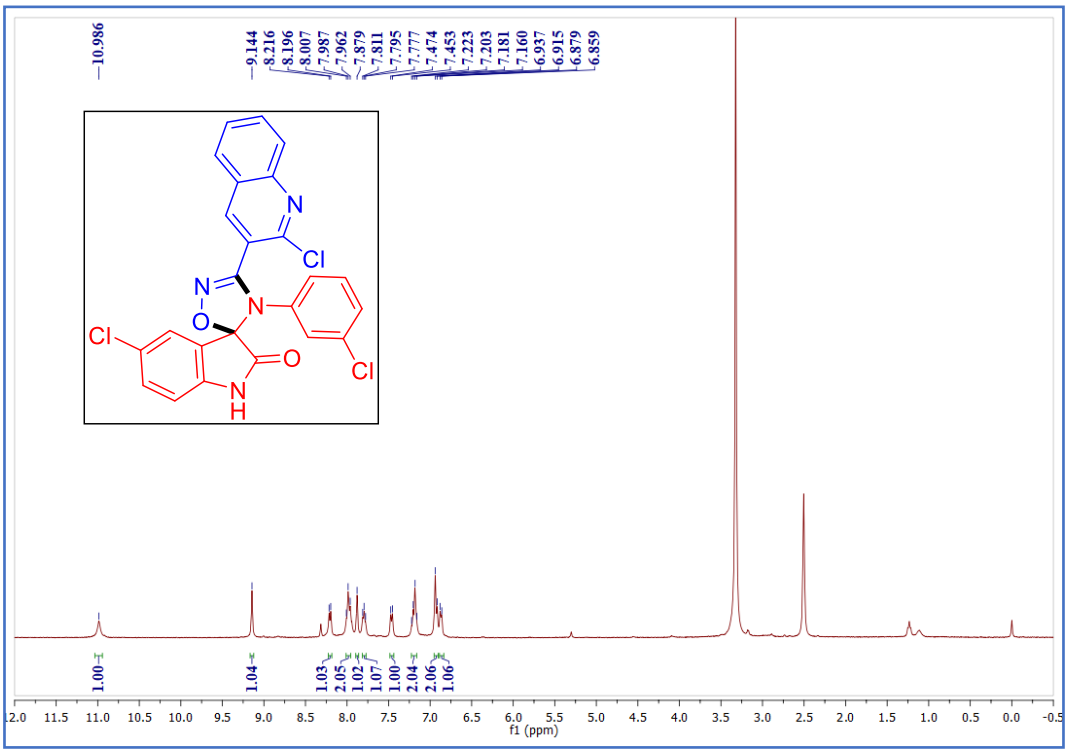

^{1}H NMR spectrum of the compound **3j**

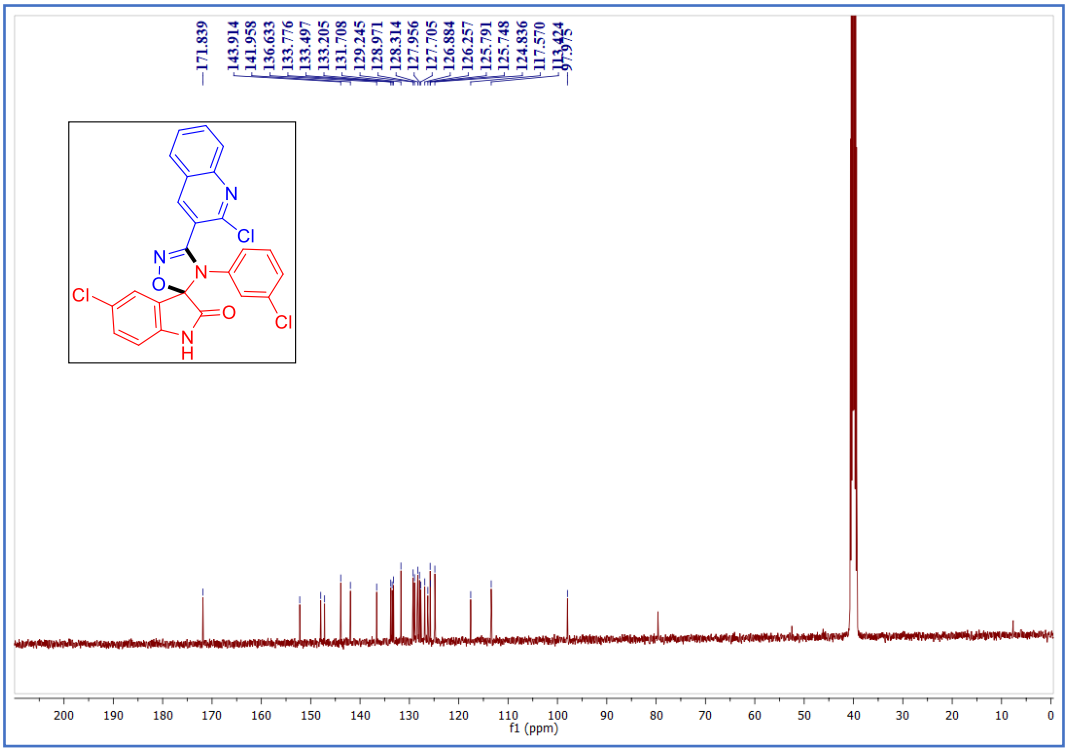

^{13}C NMR spectrum of the compound **3j**

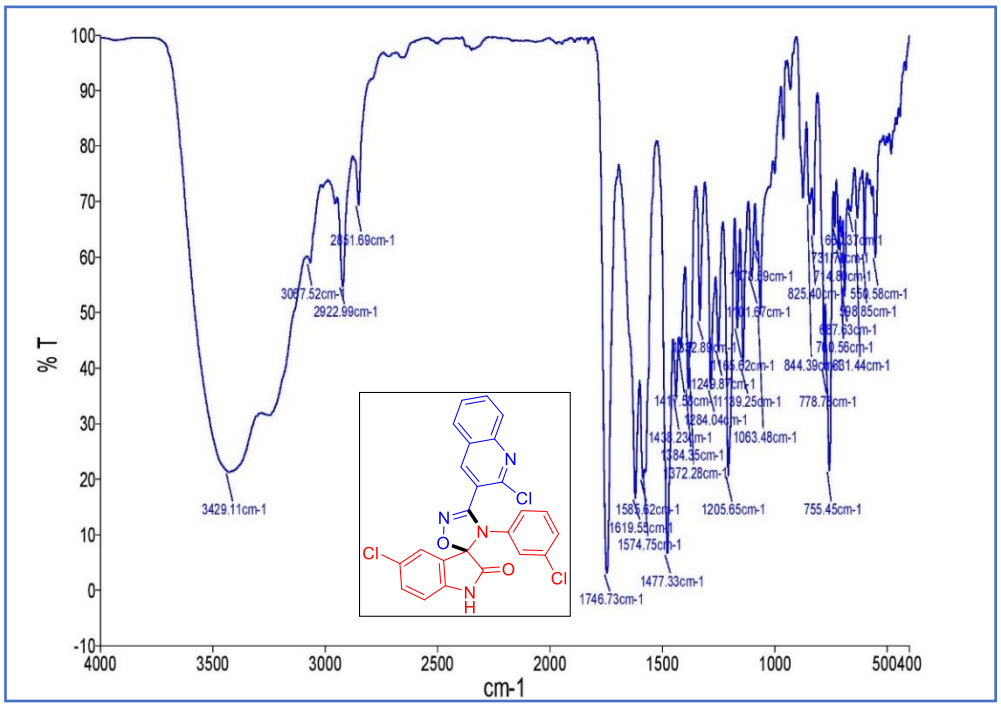

IR spectrum of the compound **3j**

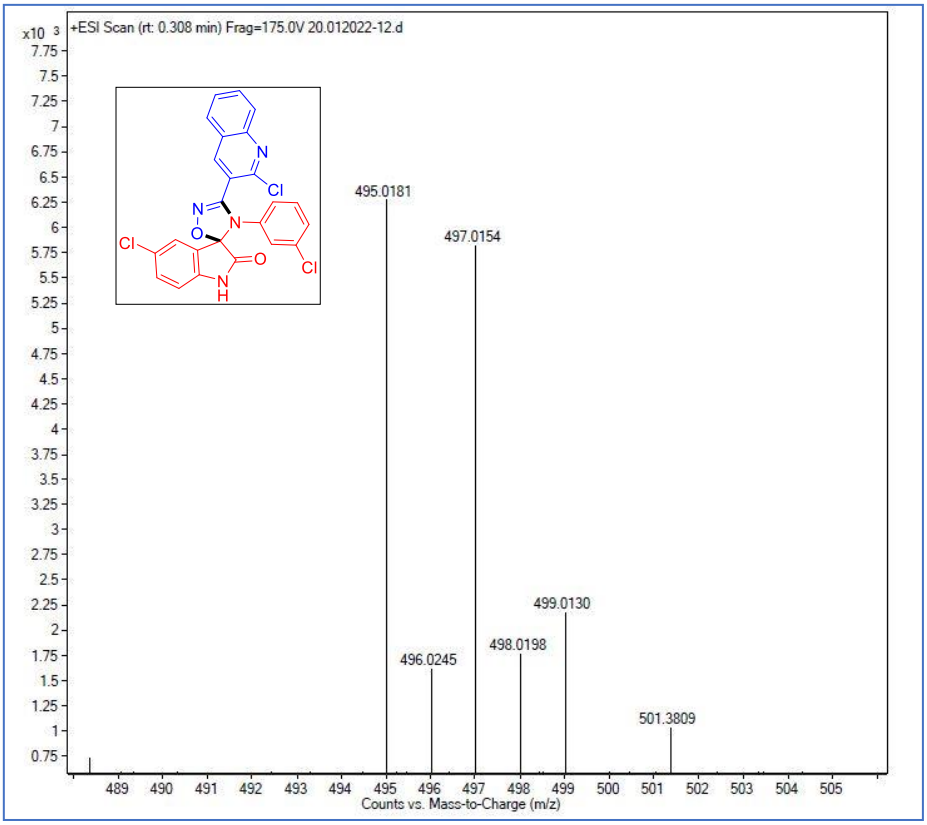

Mass spectrum of the compound **3j**

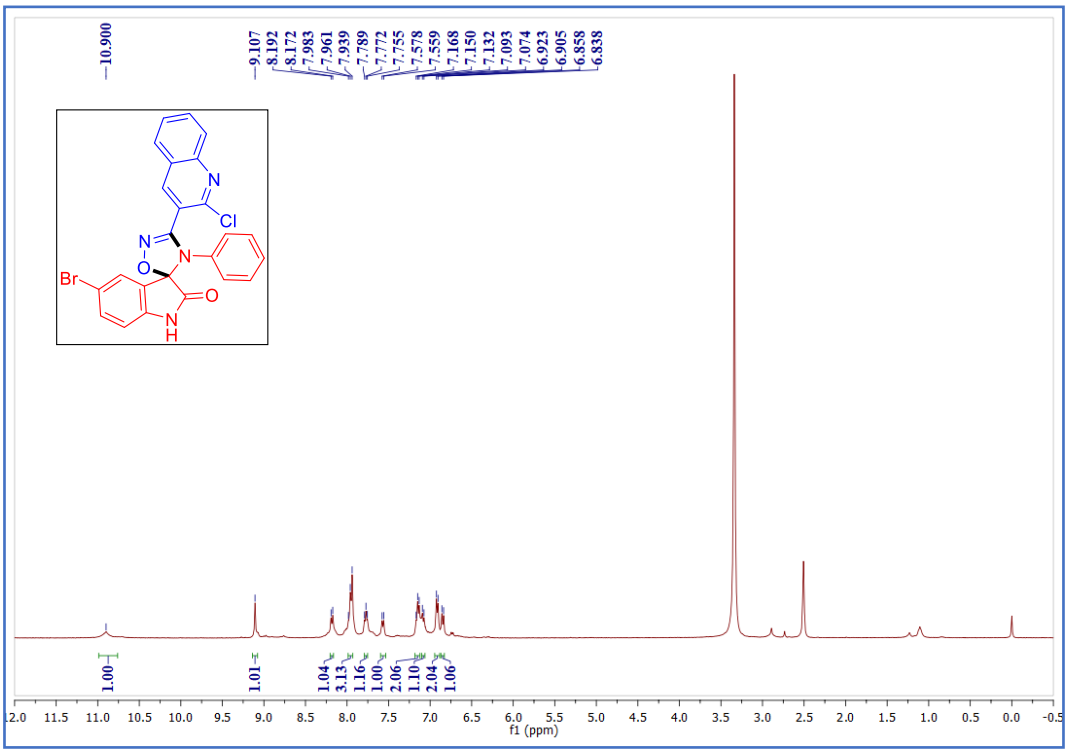

^{1}H NMR spectrum of the compound **3k**

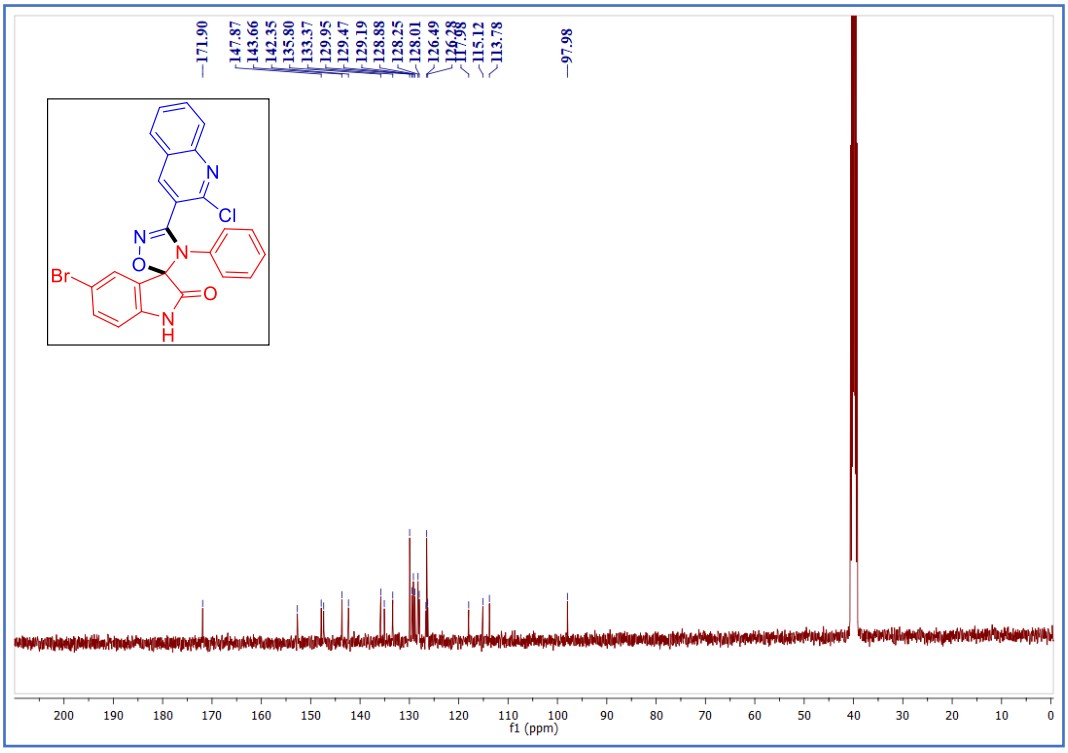

^{13}C NMR spectrum of the compound **3k**

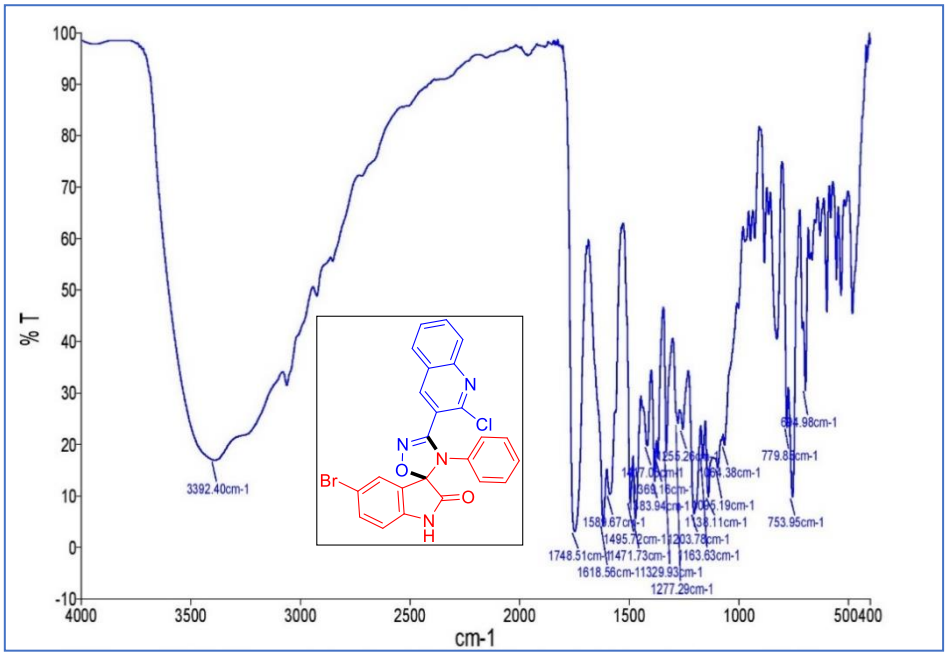

IR spectrum of the compound **3k**

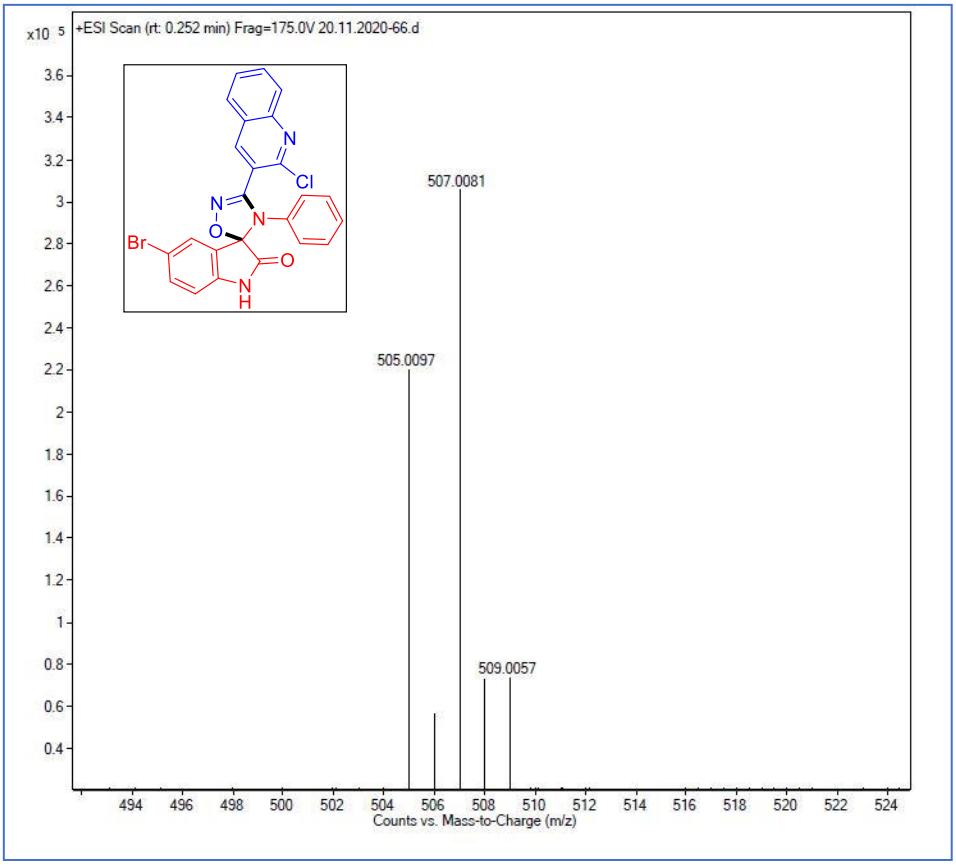

Mass spectrum of the compound **3k**

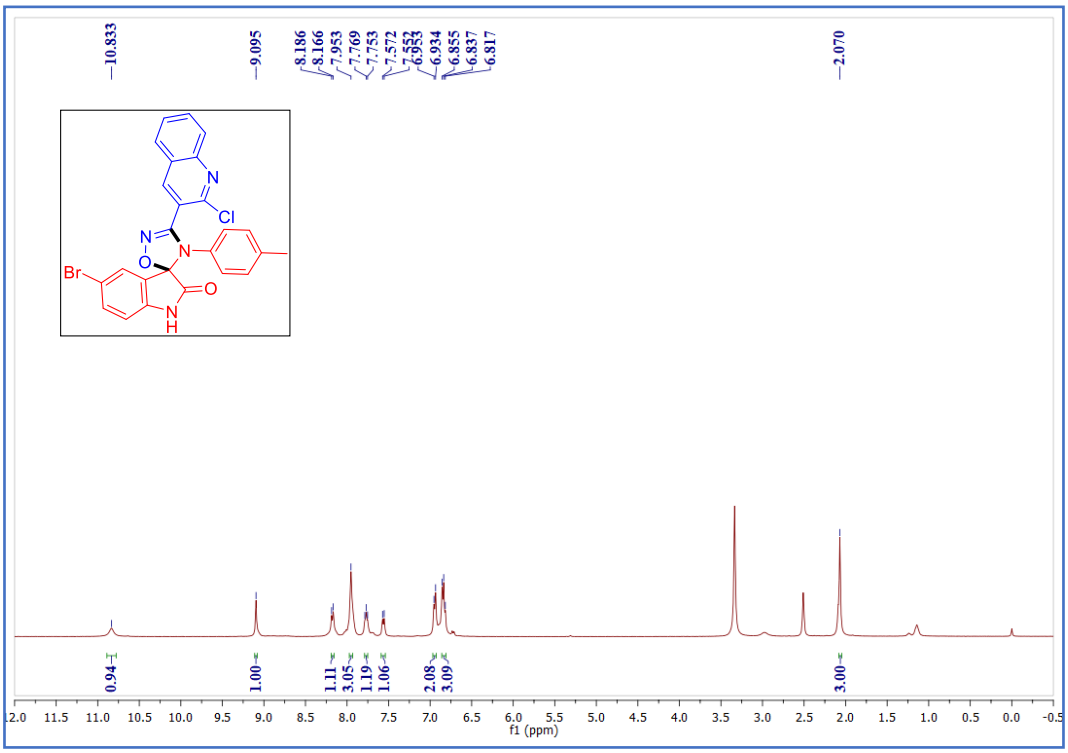

^{1}H NMR spectrum of the compound **3l**

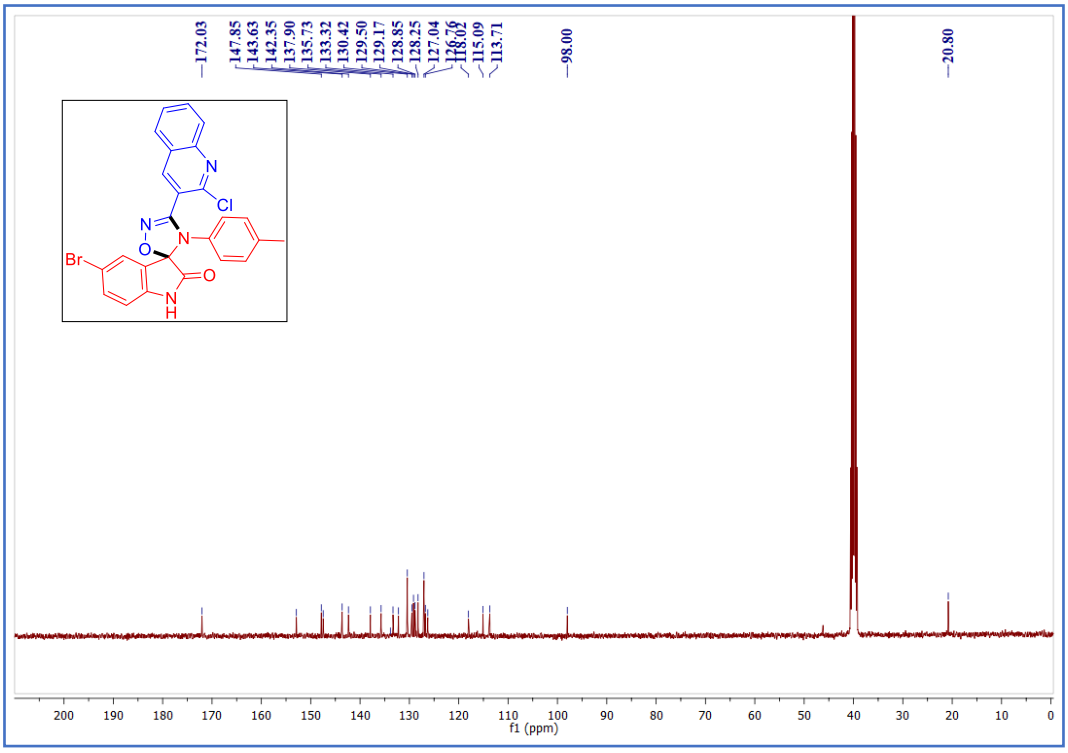

^{13}C NMR spectrum of the compound **3l**

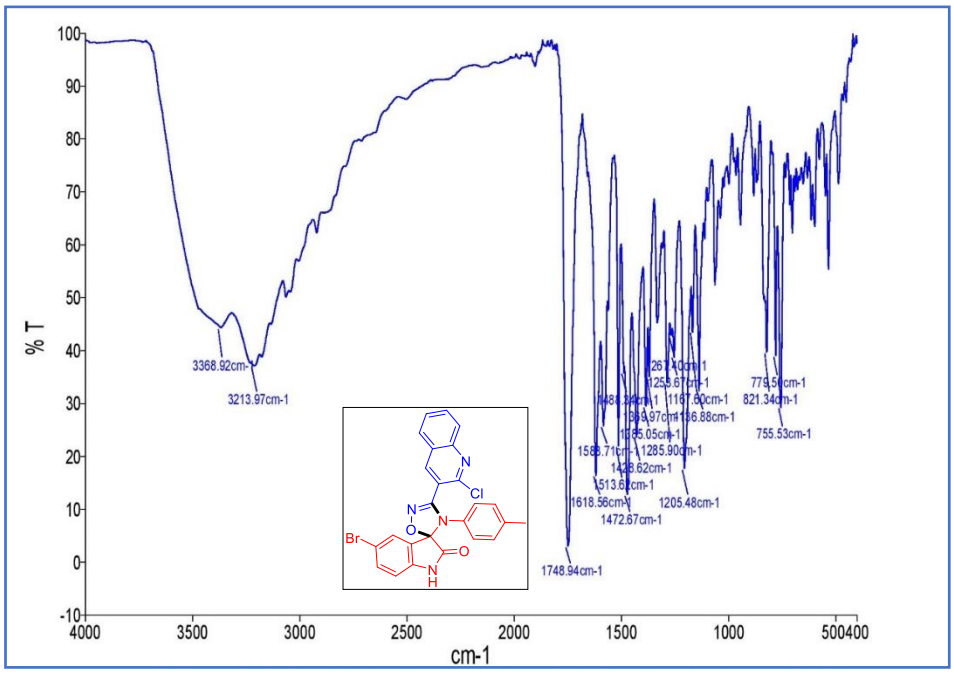

IR spectrum of the compound **3l**

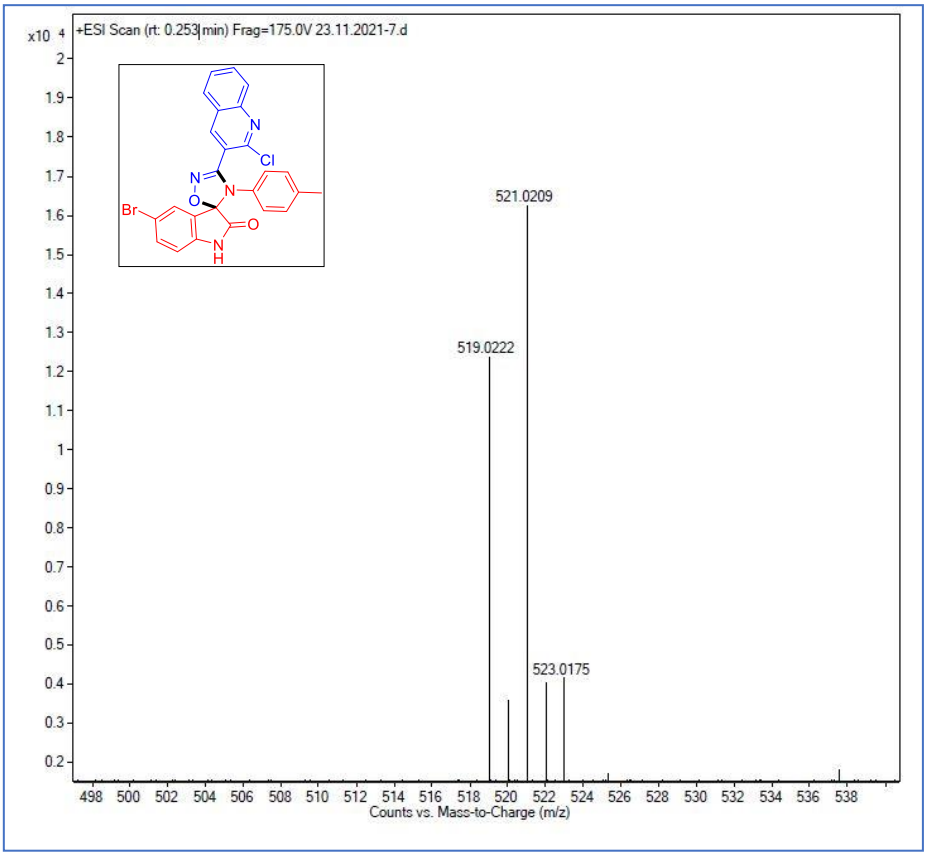

Mass spectrum of the compound **3l**

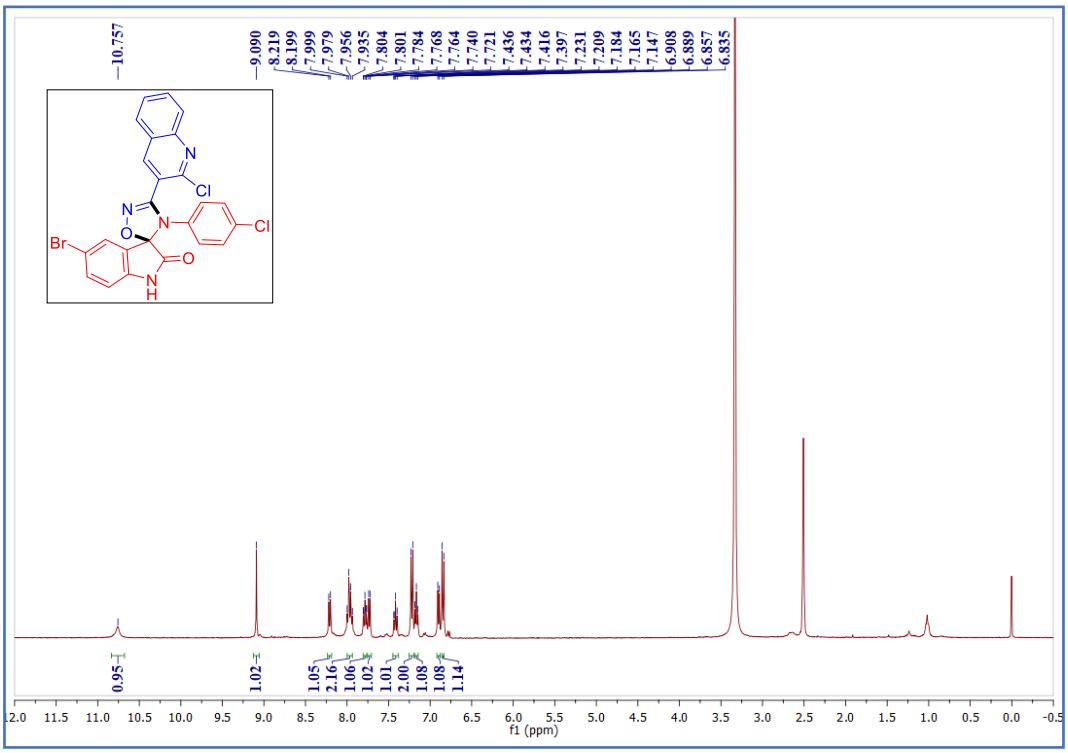

^{1}H NMR spectrum of the compound **3m**

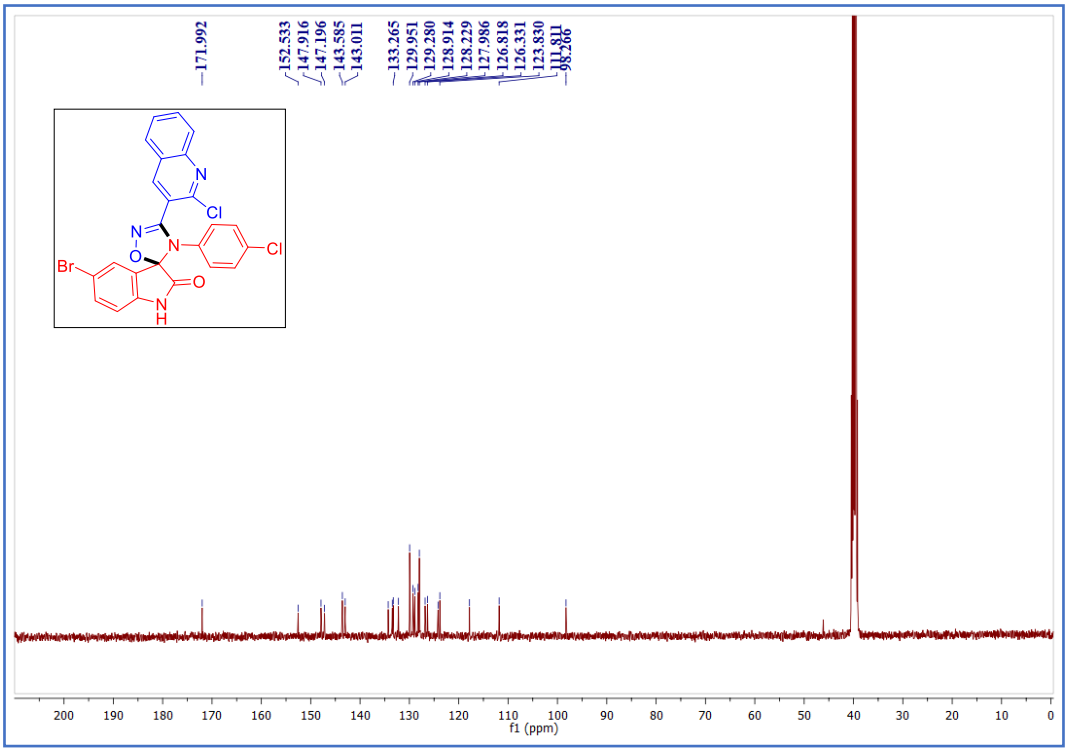

^{13}C NMR spectrum of the compound **3m**

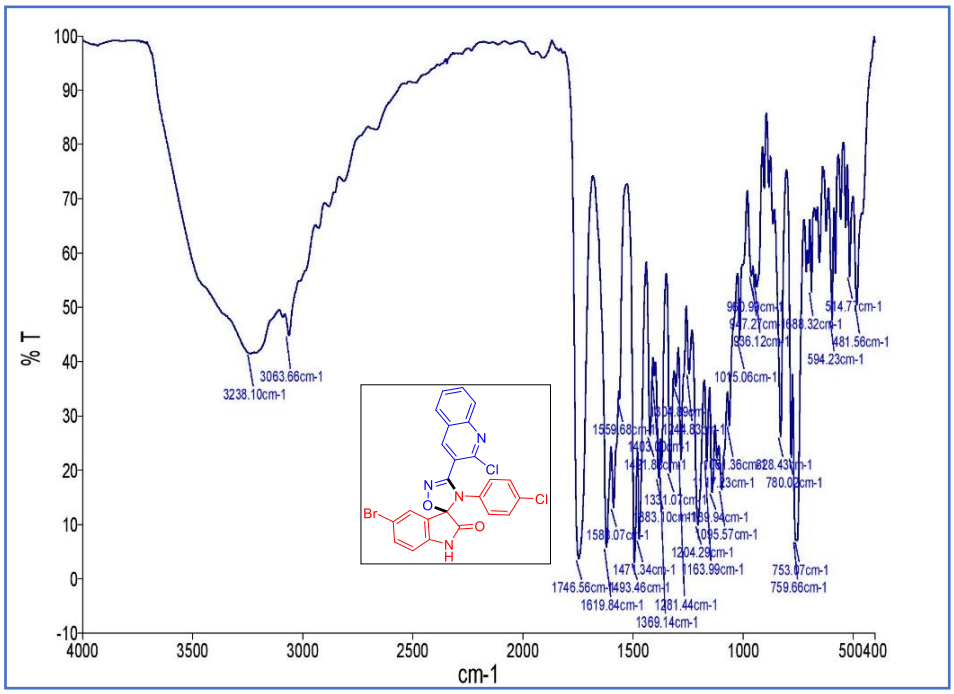

IR spectrum of the compound **3m**

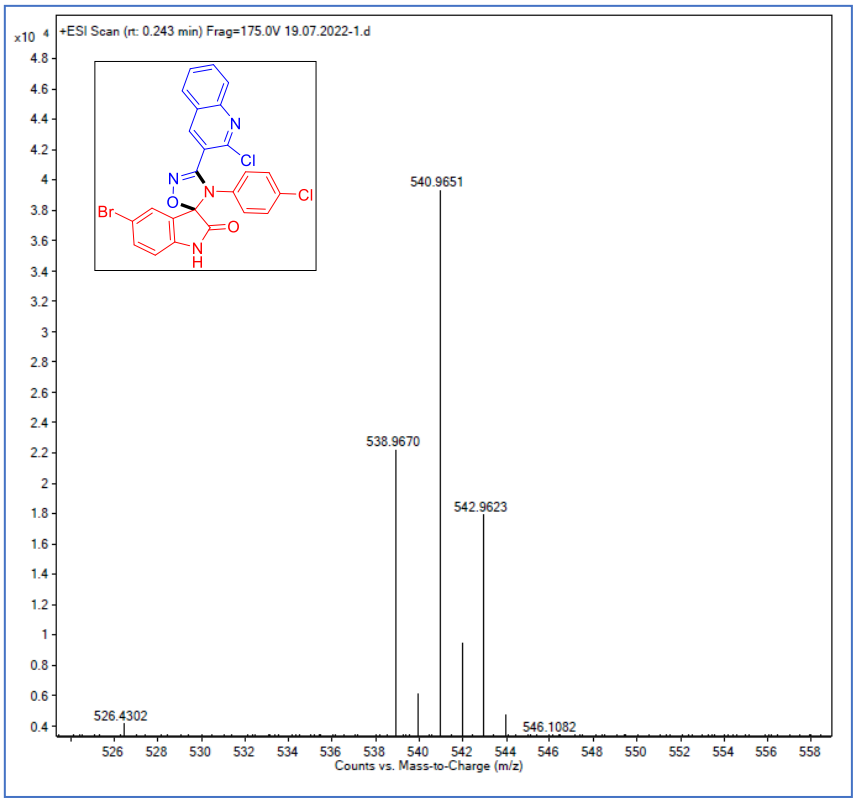

Mass spectrum of the compound **3m**

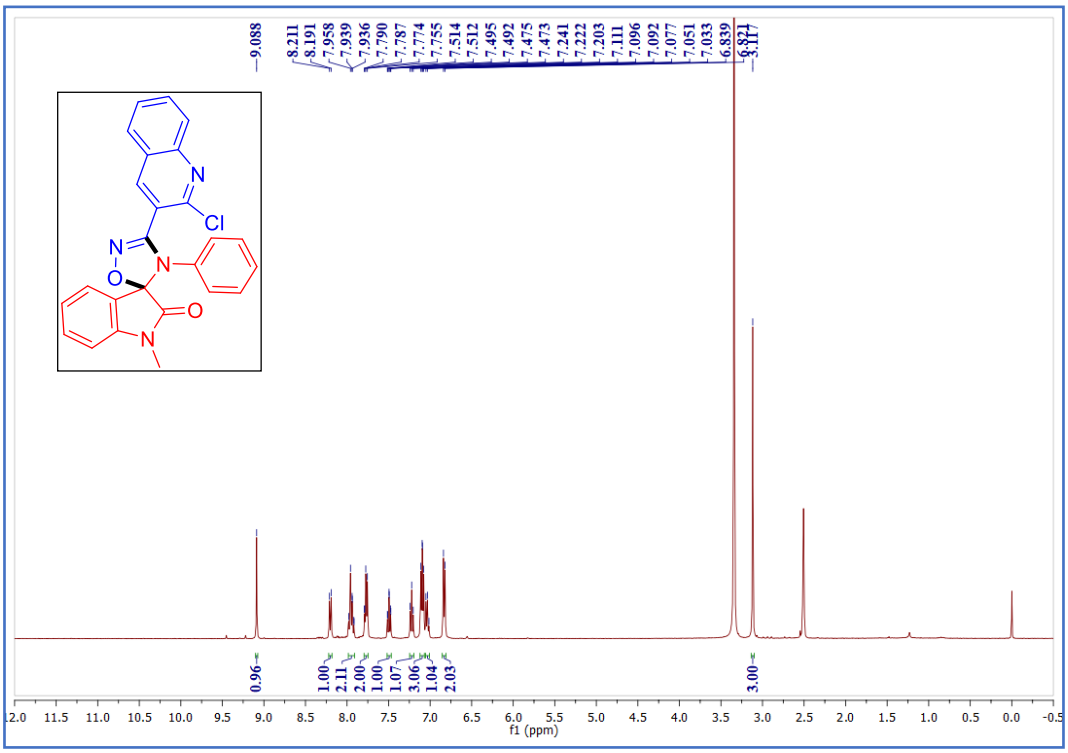

^{1}H NMR spectrum of the compound **3n**

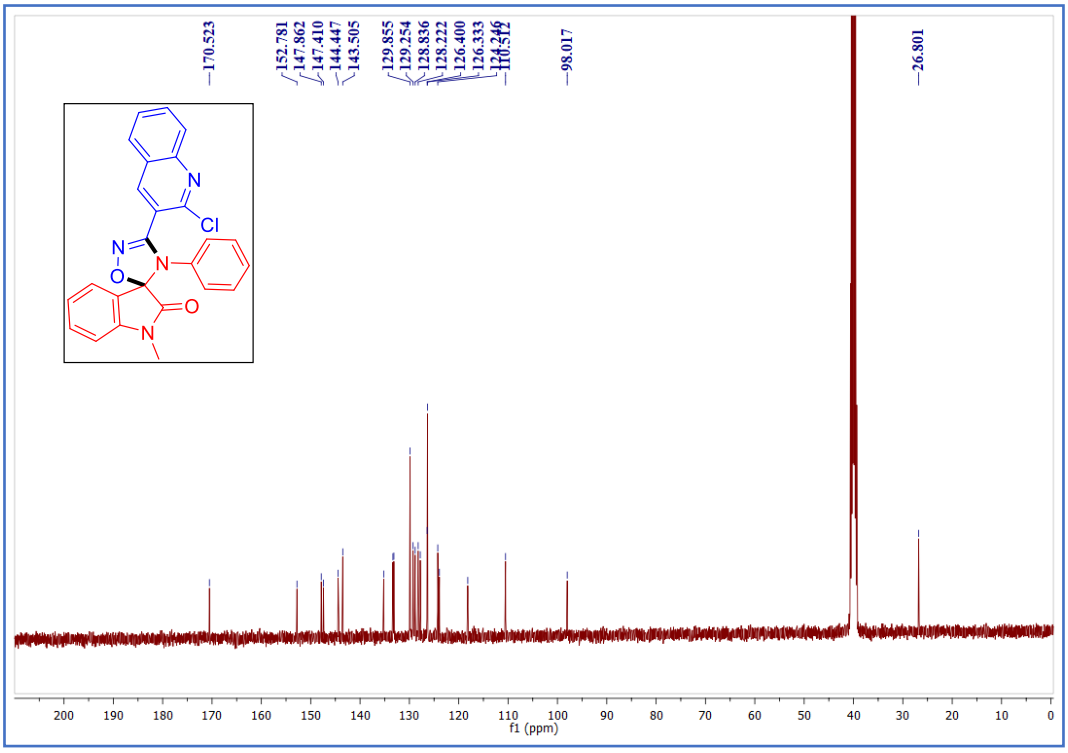

^{13}C NMR spectrum of the compound **3n**

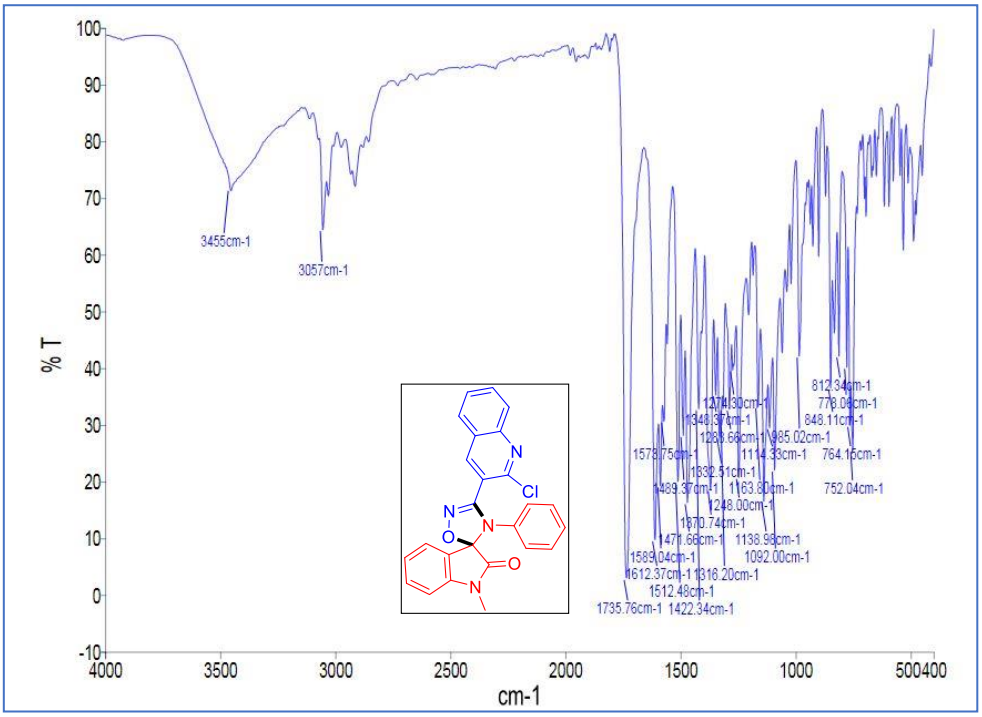

IR spectrum of the compound **3n**

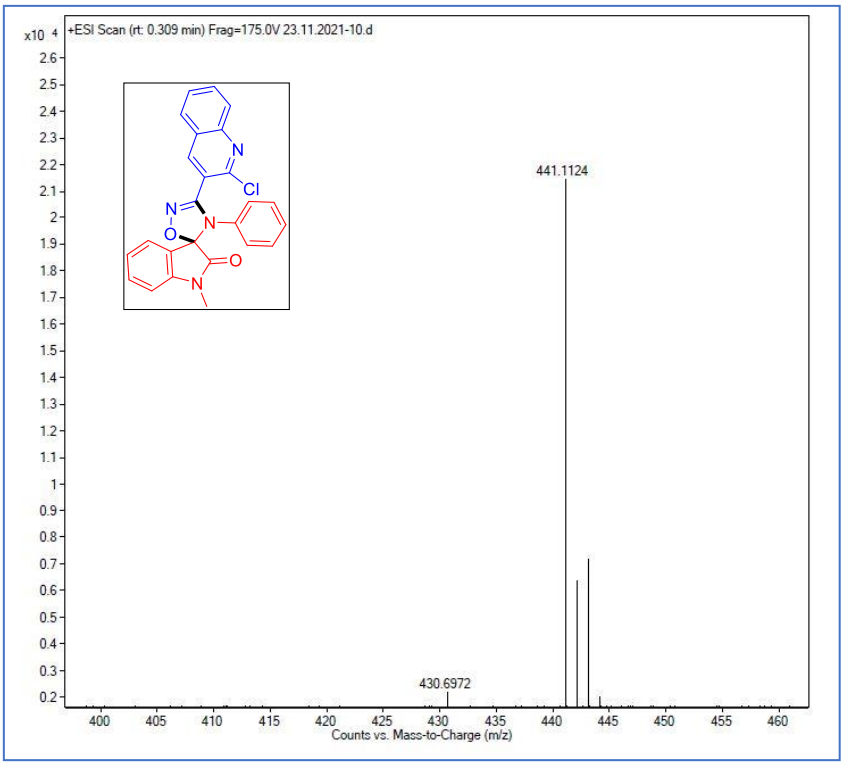

Mass spectrum of the compound **3n**

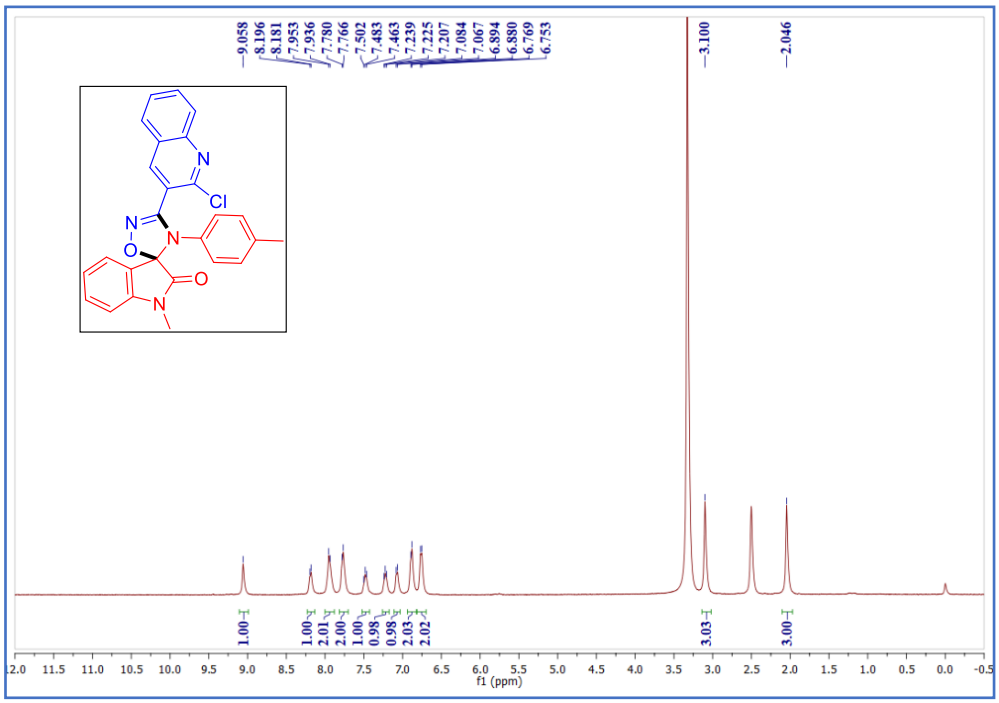

^{1}H NMR spectrum of the compound **3o**

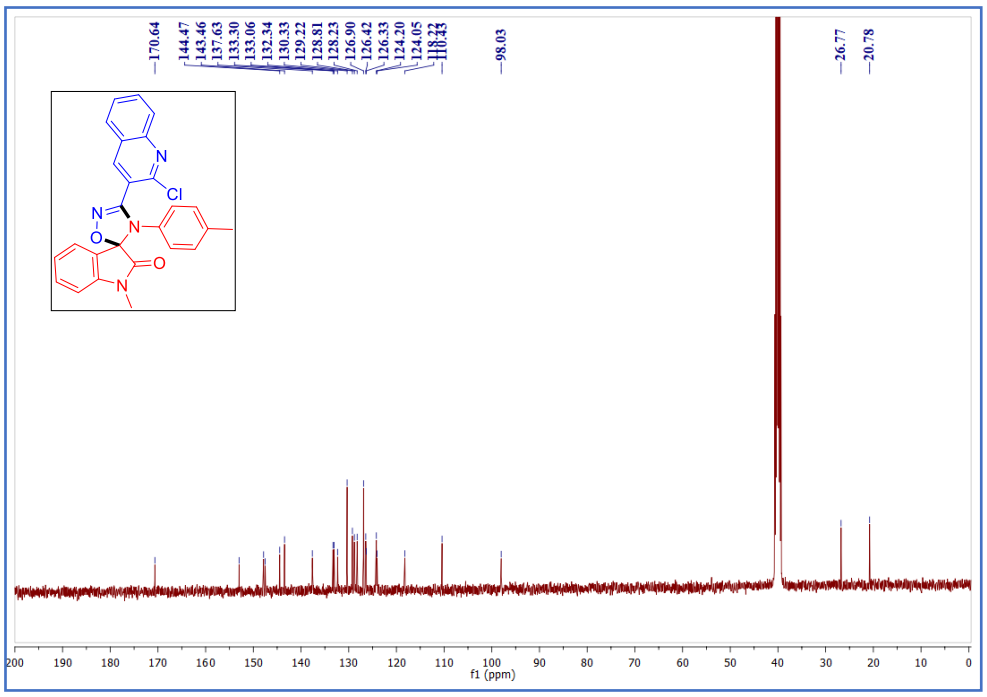

^{13}C NMR spectrum of the compound **3o**

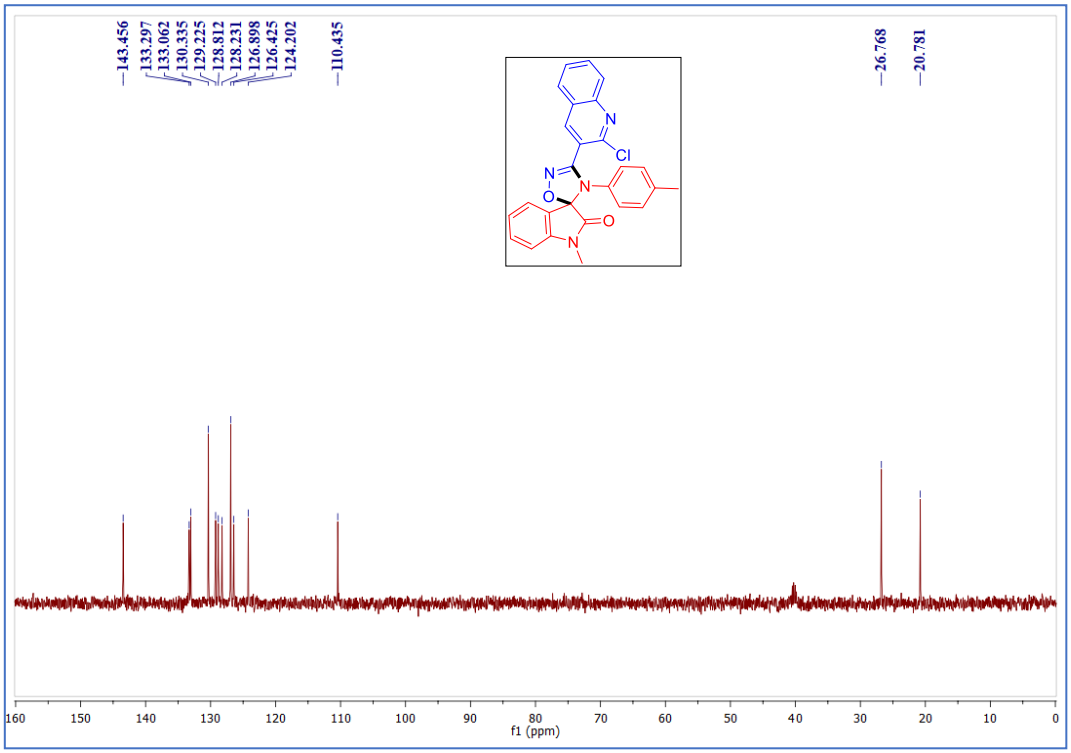

DEPT135 spectrum of the compound **3o**

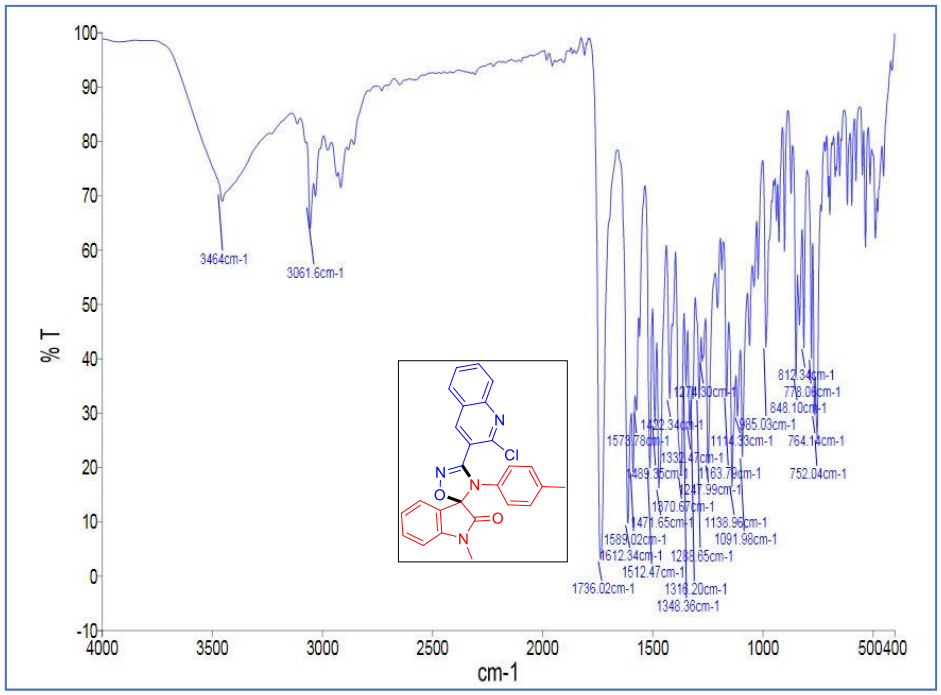

IR spectrum of the compound **3o**

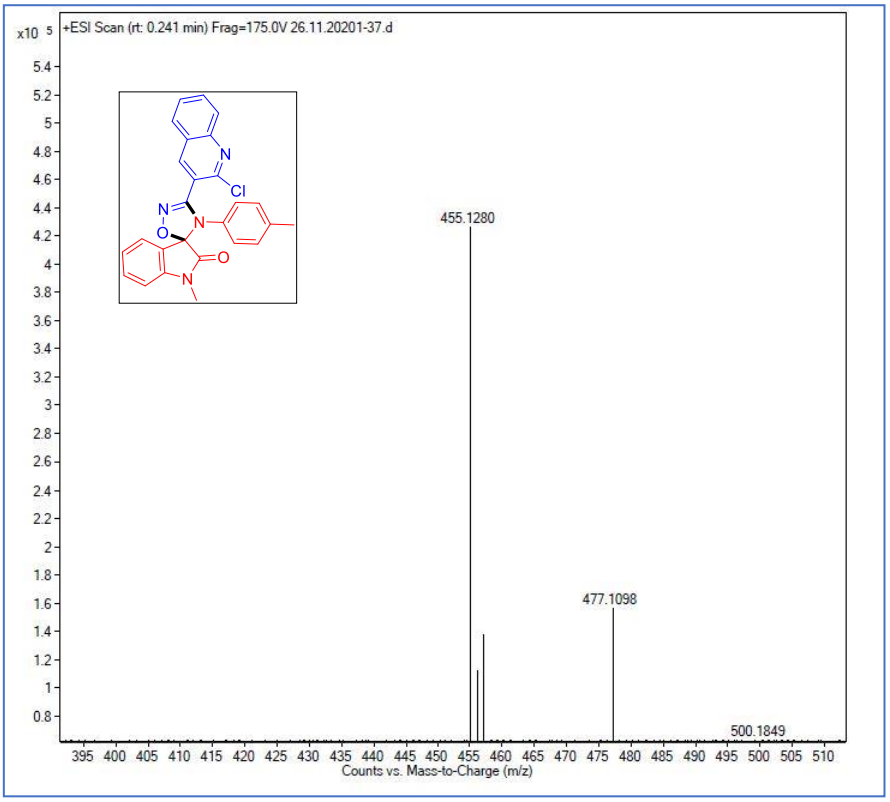

Mass spectrum of the compound **3o**

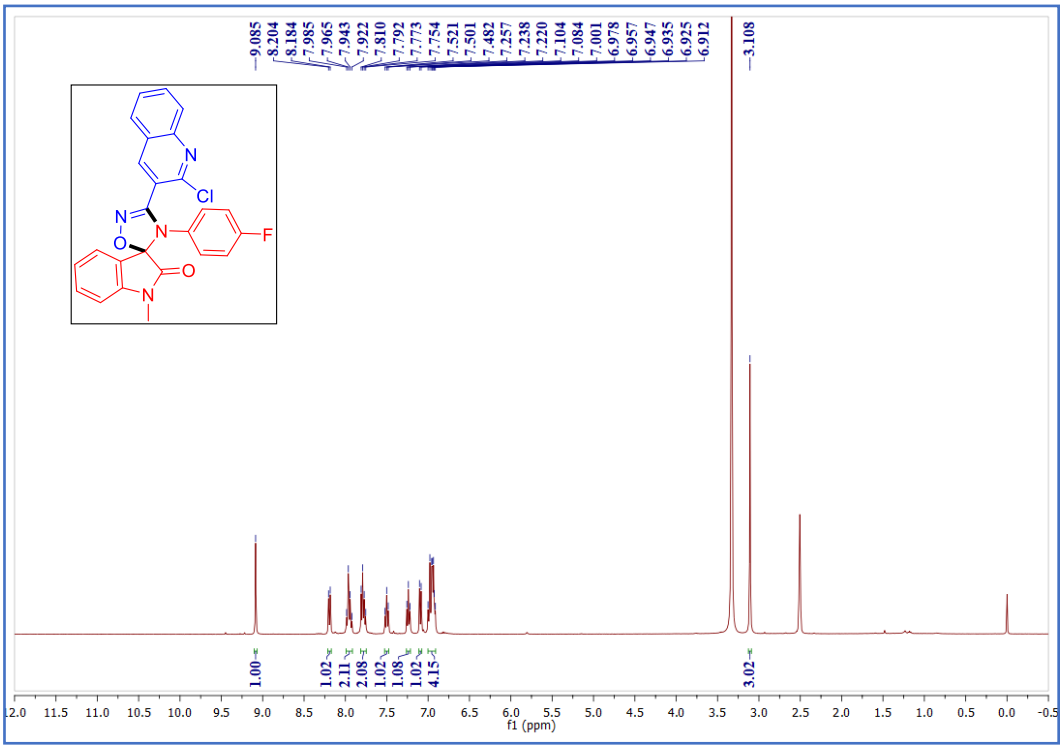

^{1}H NMR spectrum of the compound **3p**

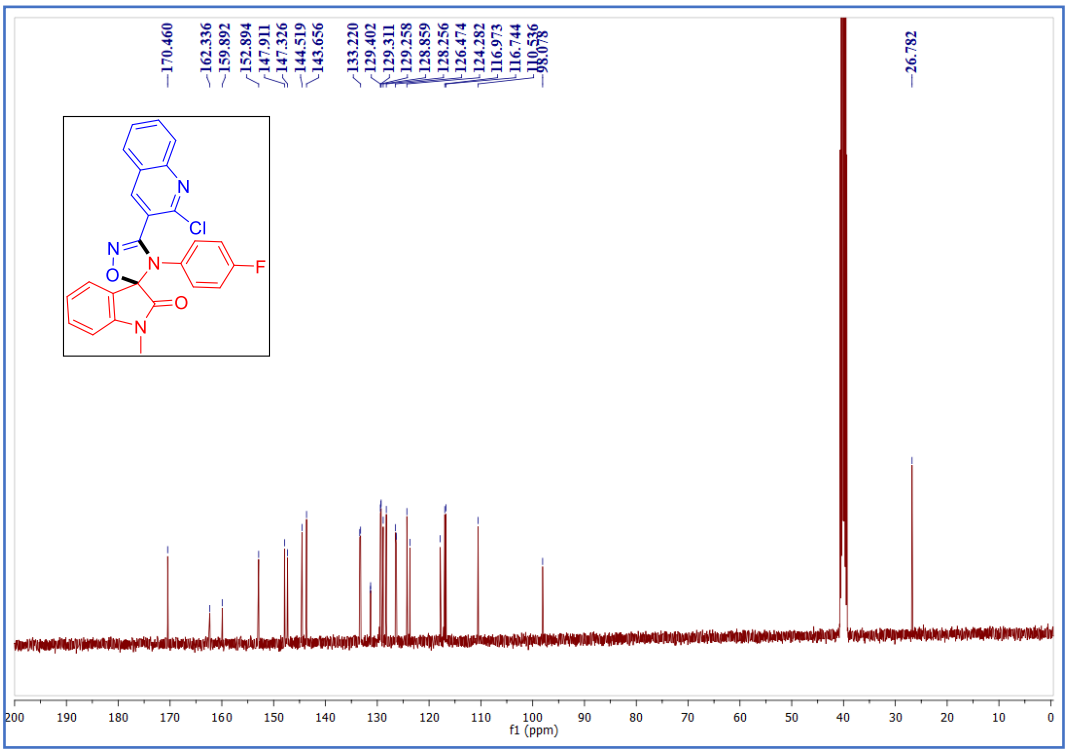

^{13}C NMR spectrum of the compound **3p**

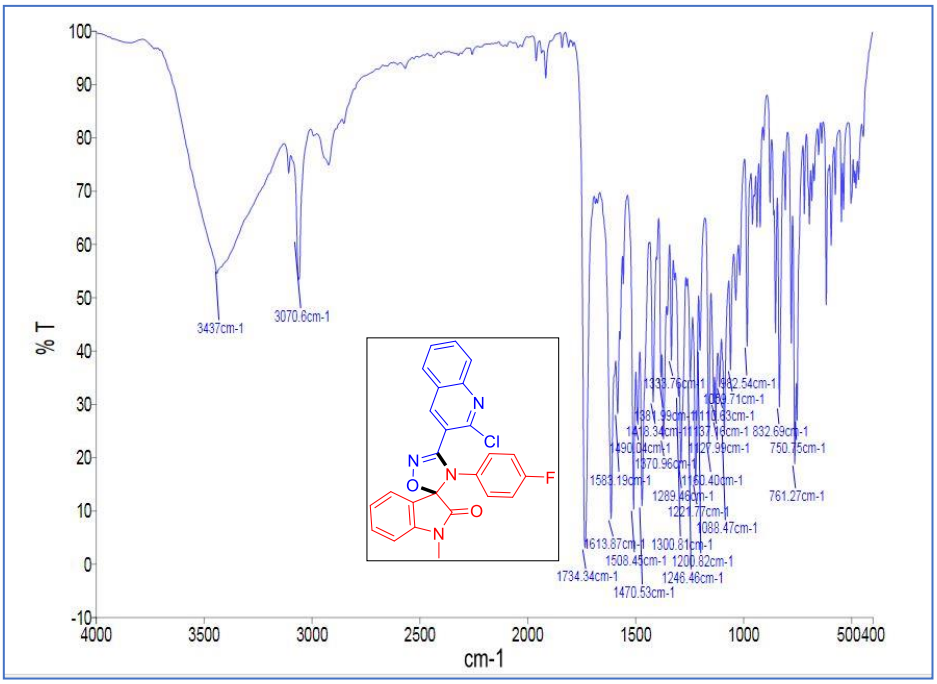

IR spectrum of the compound **3p**

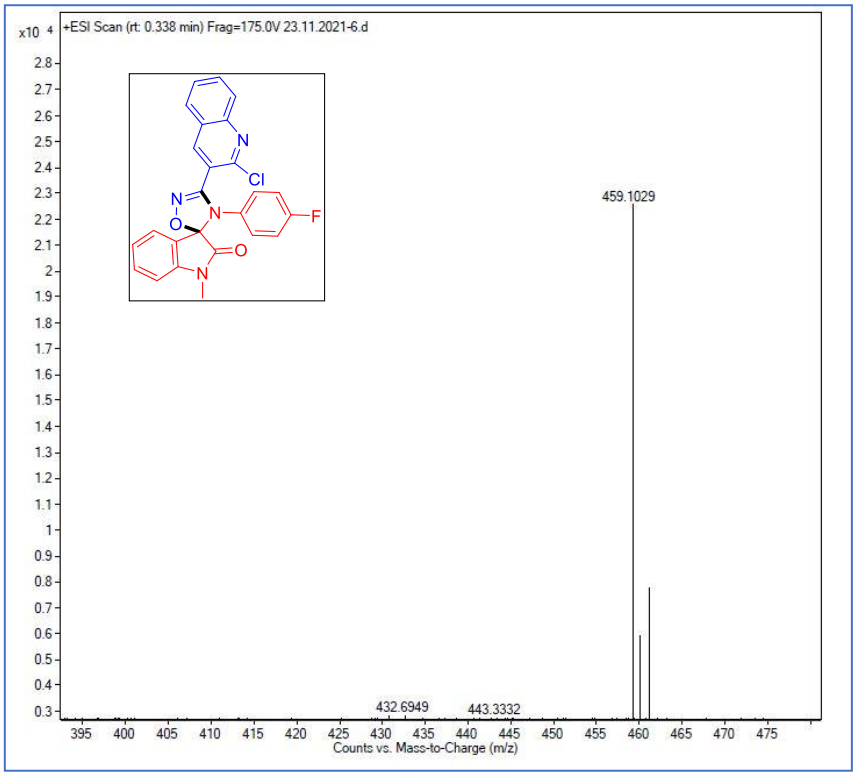

Mass spectrum of the compound **3p**

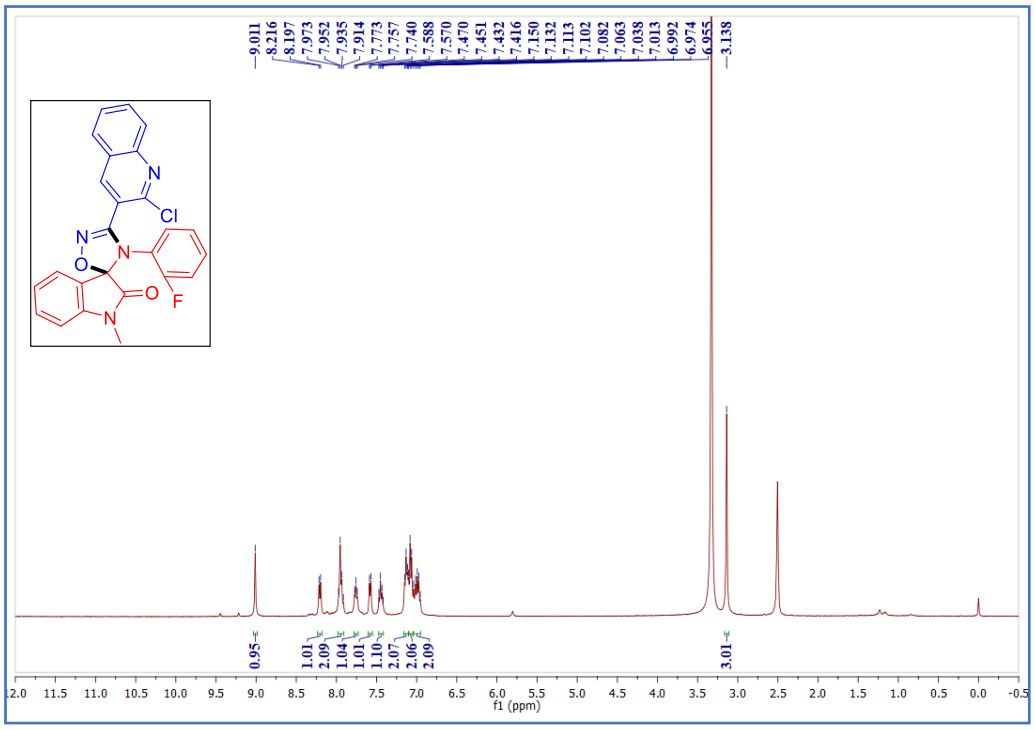

^{1}H NMR spectrum of the compound **3q**

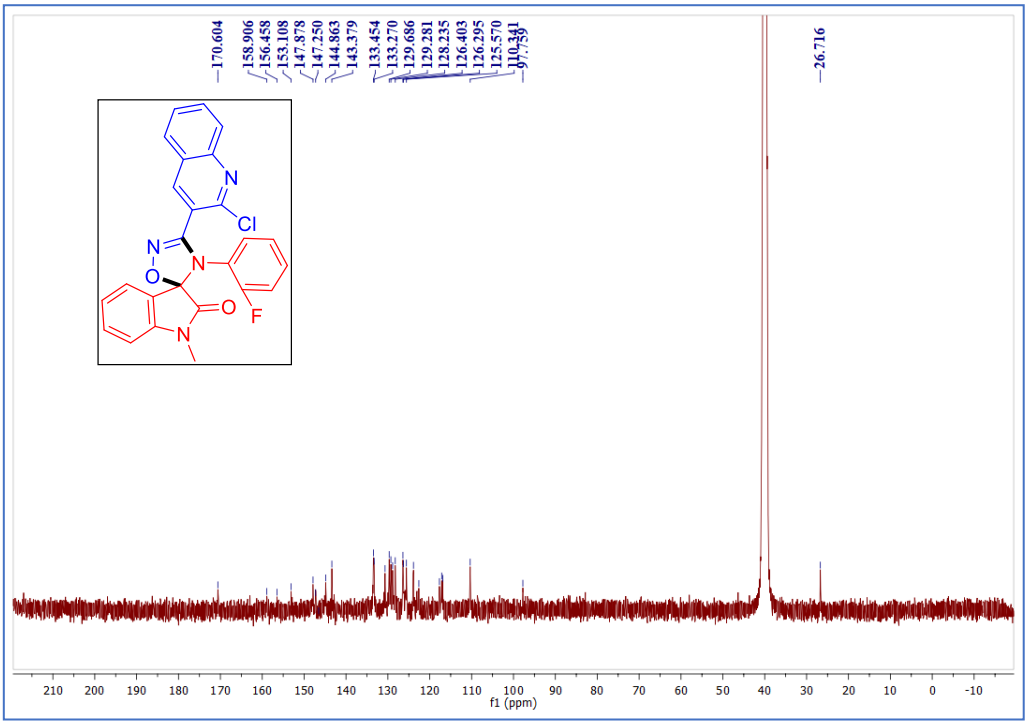

^{13}C NMR spectrum of the compound **3q**

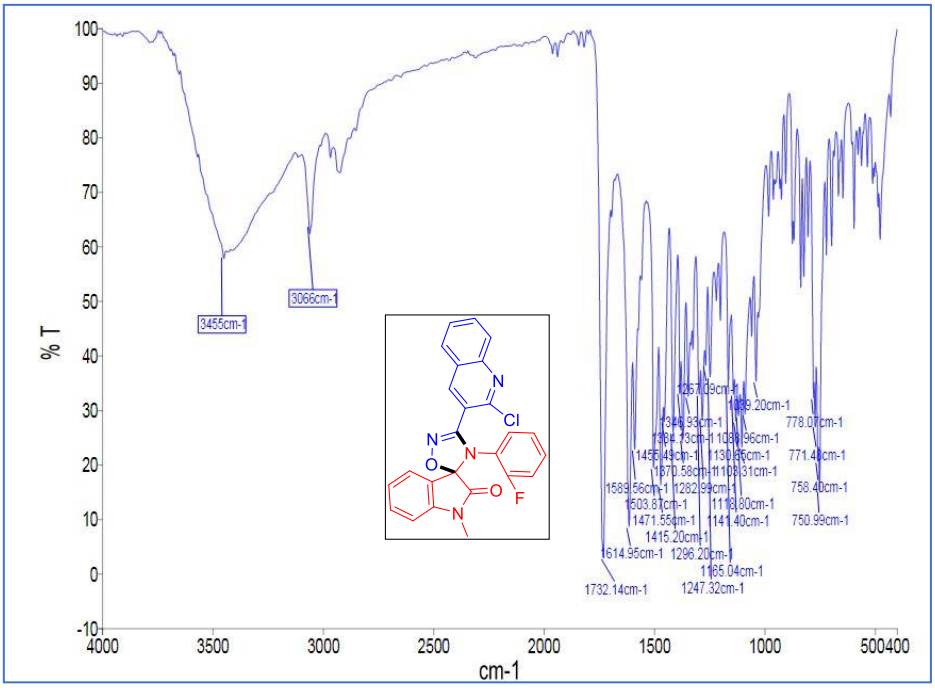

IR spectrum of the compound **3q**

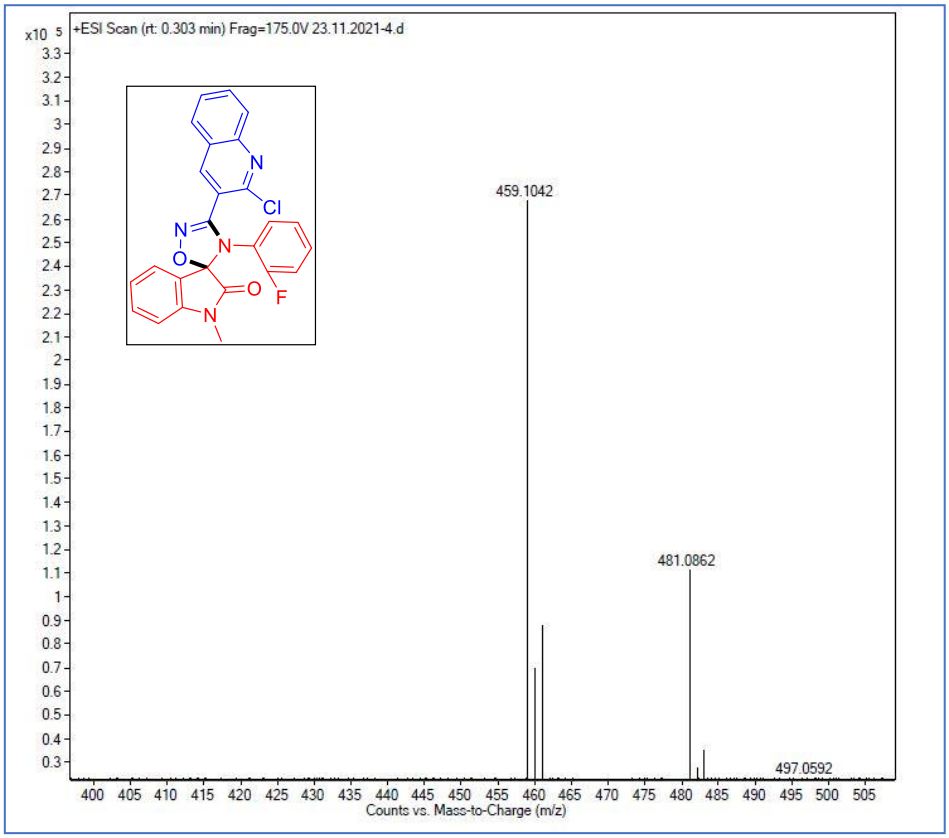

Mass spectrum of the compound **3q**

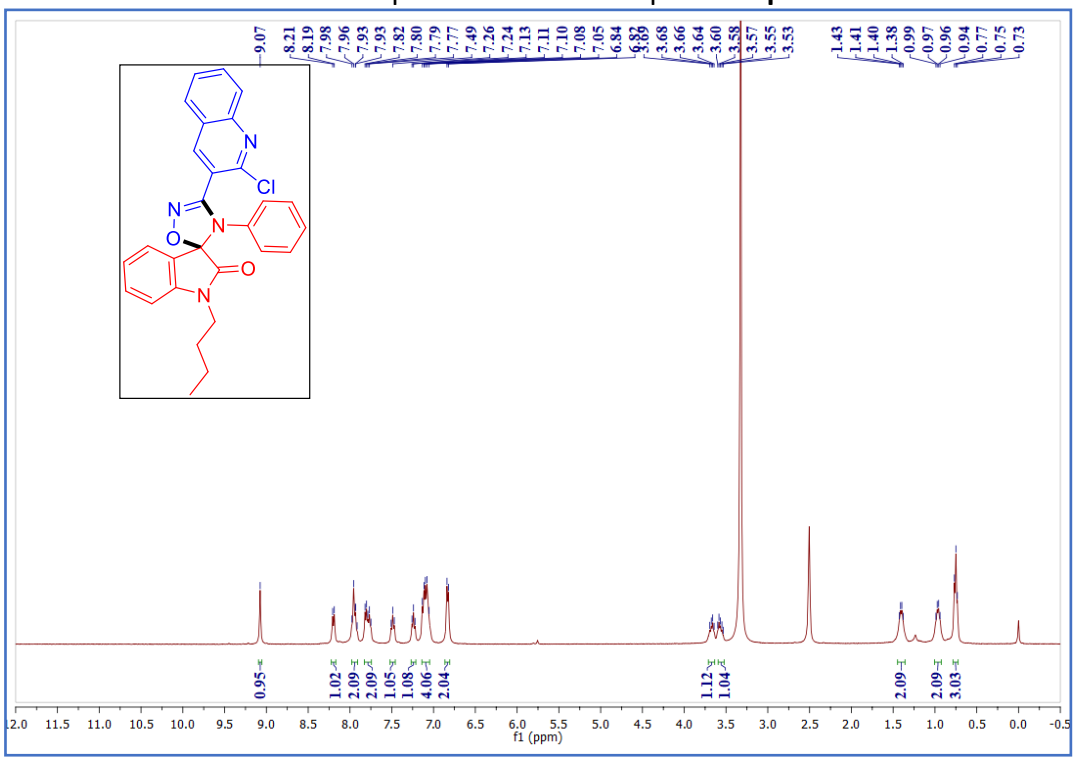

^{1}H NMR spectrum of the compound **3r**

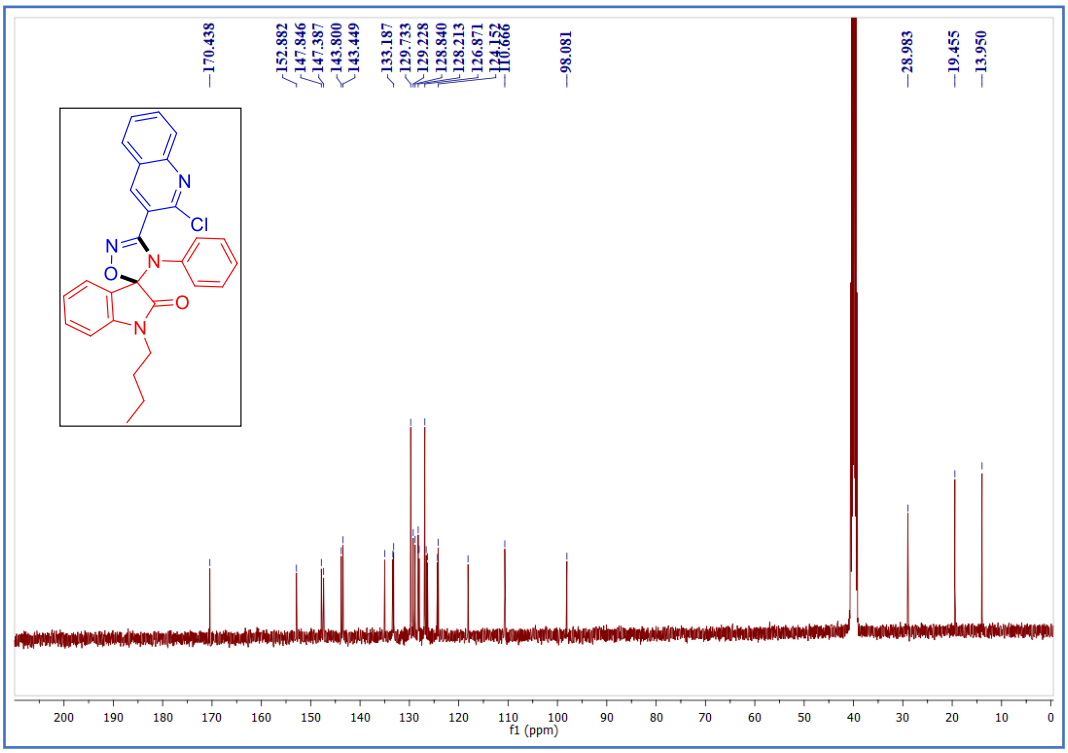

^{13}C NMR spectrum of the compound **3r**

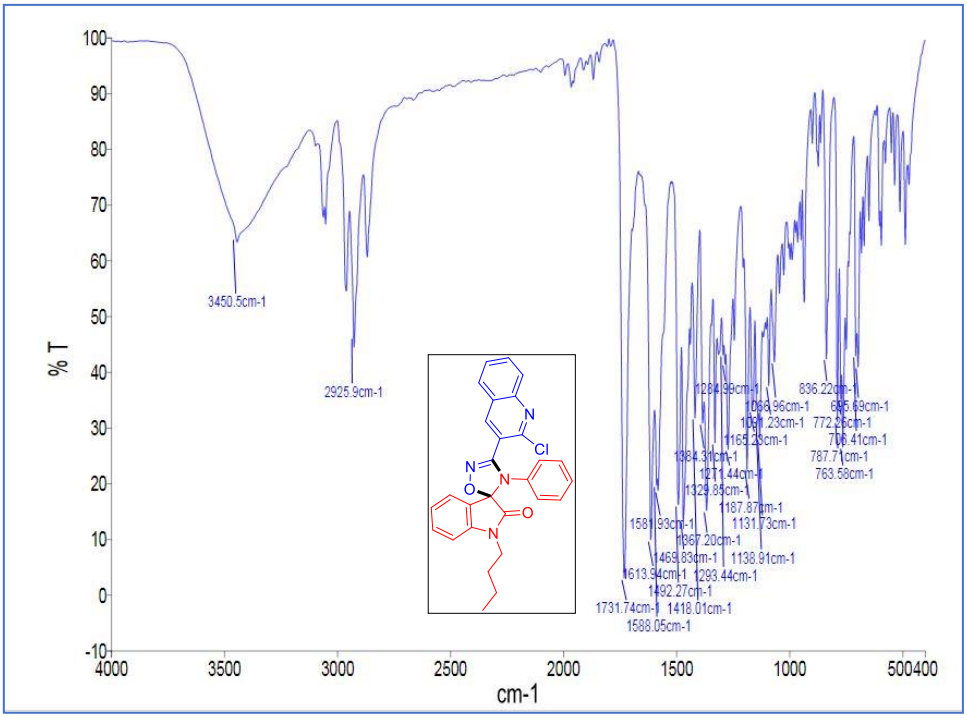

IR spectrum of the compound **3r**

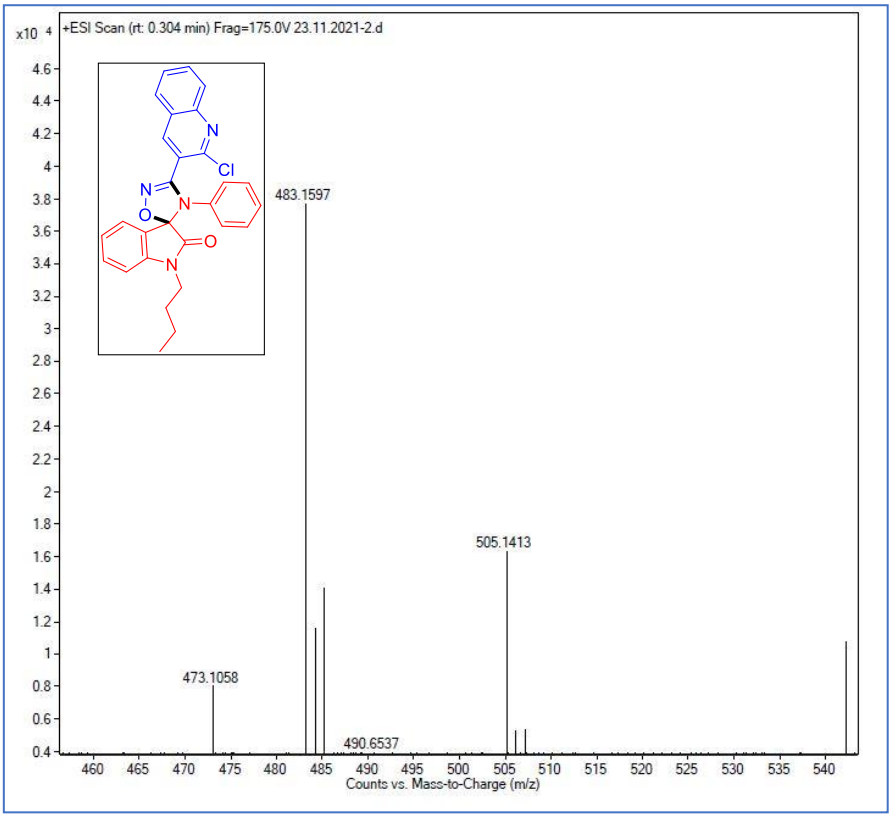

Mass spectrum of the compound **3r**

2. Salient features of crystallographic data of compound 3r

	3r
Empirical formula	$C_{28}H_{23}ClN_4O_2$
Formula weight	482.9680
Crystal system	Orthorhombic
Space group	*I*-21
T/K	100(2)
a/Å	21.0338(12)
b/Å	16.4531(11)
c/Å	6.8629(5)
α/°	90
β/°	90
γ/ °	90
Z	4
V/Å^3	2375.1(3)
D_{calc}/ g/cm^3	1.356
F(000)	1016.0
μ/mm^{-1}	0.195
ϑ/º	1.936 to 26.999
Index ranges	-26 ≤ *h* ≤ 26

	$-21 \le k \le 21$ $-8 \le l \le 8$
N-total	107312
N-independent	5184
N-observed	5064
Parameters	318
R_1 ($I > 2\sigma(I)$)	0.0331
wR_2 (all data)	0.0987
GOF	1.105
CCDC	2222697

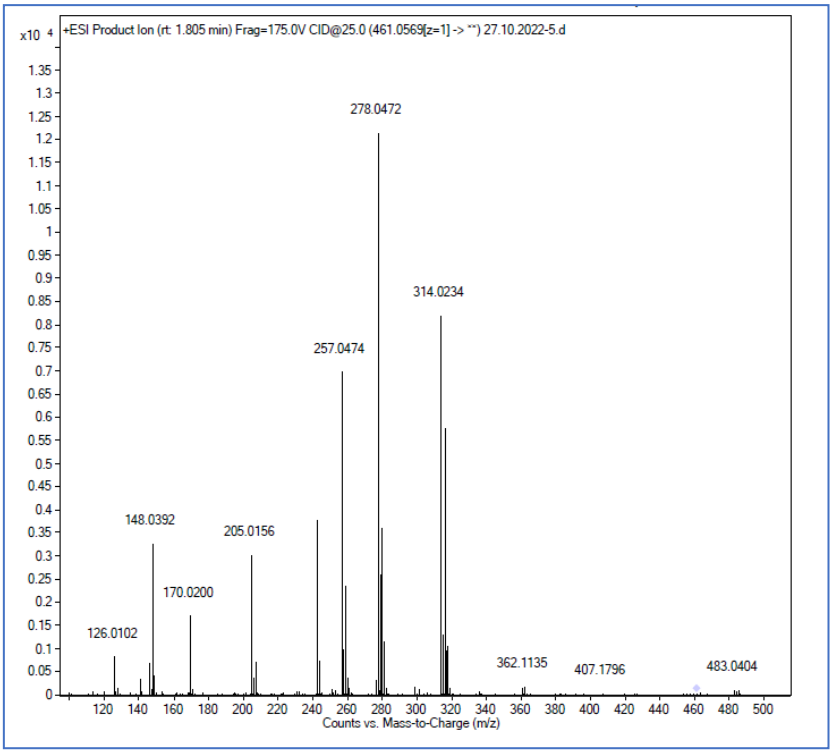

Fragmentation pathway of the compound **3e**

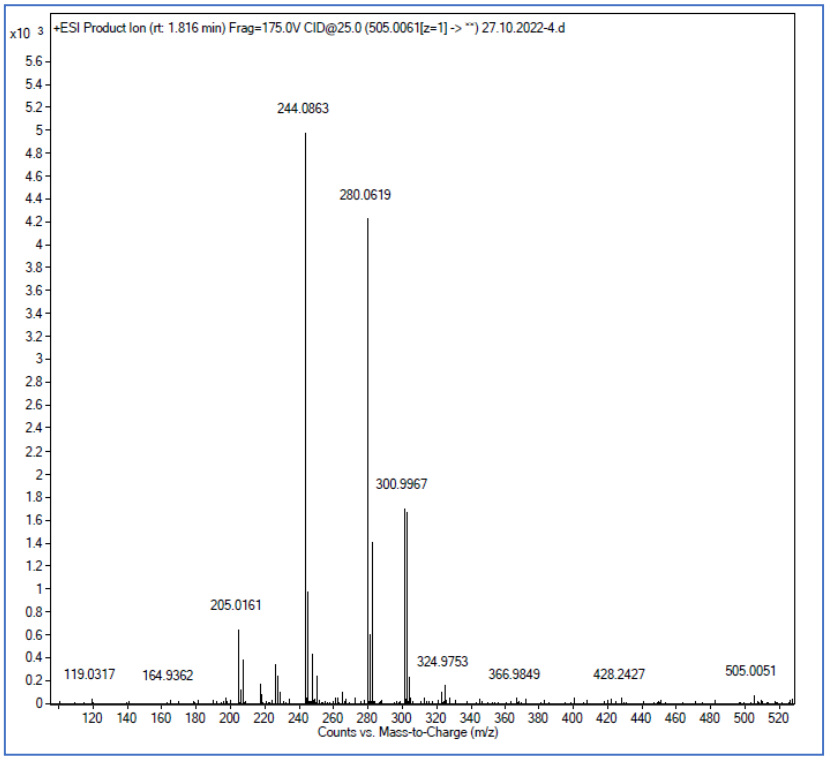

Fragmentation pathway of the compound **3k**

3. Biological evaluation

Table S1. IC_{50} values[a] (in μM) for compounds **3a-r**

Compound	SK-OV-3[b]	HeLa[c]	HCT-116[d]	DU-145[e]	A549[f]	HEK-293[g]
3a	51.80±1.81	49.51±2.34	74.68±3.35	57.76±2.38	58.06±1.92	> 100 (110.27±4.23)
3b	33.98±2.83	31.08±2.78	67.62±2.90	39.19±3.59	51.21±1.98	92.56±1.22
3c	58.23±4.68	42.84±3.79	85.60±2.06	65.56±4.02	59.86±3.71	> 100 (103.26±2.80)
3d	21.27±0.13	**16.61±0.61**	52.96±2.82	28.63±2.20	48.07±3.35	99.10±3.73
3e	26.47±1.95	21.62±0.95	51.44±2.58	33.71±1.52	53.11±1.51	74.88±4.40
3f	48.72±4.85	38.10±2.13	69.04±3.72	43.58±2.92	48.40±1.18	> 100 (108.62±4.37)
3g	24.14±0.49	20.28±0.98	66.53±2.90	36.34±0.97	43.65±4.72	89.69±3.02
3h	**18.81±0.75**	**15.14±0.96**	53.71±3.65	25.55±2.08	36.01±1.28	98.70±4.87
3i	**14.35±0.14**	**10.75±0.39**	61.24±4.05	**19.27±0.62**	34.75±1.28	> 100 (106.07±1.62)
3j	20.53±1.37	**12.43±0.77**	54.85±2.71	26.28±1.98	37.26±1.08	92.97±3.72
3k	25.10±1.22	**18.80±1.54**	64.26±4.38	31.84±1.79	40.96±2.49	> 100 (120.51±3.91)
3l	27.37±1.74	22.08±0.22	71.85±4.29	33.93±3.14	55.73±3.90	> 100 (108.77±2.50)
3m	45.48±1.47	35.61±1.91	67.34±4.75	42.85±0.79	71.14±3.57	89.32±0.80
3n	23.99±1.71	**18.53±0.91**	51.29±3.10	39.09±2.58	62.22±4.86	> 100 (108.56±1.67)
3o	31.88±1.65	24.74±1.03	53.94±0.39	28.85±1.60	43.19±2.64	97.81±4.35
3p	**19.41±1.22**	**16.69±1.15**	48.72±1.87	24.81±1.38	42.17±2.03	91.93±2.64
3q	51.28±3.75	36.07±3.31	71.21±3.78	69.11±2.26	48.75±1.69	> 100 (110.45±4.74)
3r	50.98±3.15	45.71±3.58	70.26±0.92	46.39±3.48	57.35±3.07	95.40±3.79
Doxorubicin	1.41±0.18	1.73±0.08	1.53±0.09	1.89±0.09	2.11±0.16	ND

[a]50% Inhibitory concentration after 48 h of drug treatment. [b]Ovarian cancer cells. [c]Cervical cancer cells. [d]Colon cancer cells. [e]Prostate cancer cells. [f]Lung cancer cells. [g]Normal Human embryonic kidney 293 cells. ND: Not determined.

4. Structure-activity relationship (SAR) studies

From the results in table S1, it was observed that the anti-cancer activity of the title compounds having 5-chloroisatin and 5-fluoroisatin showed better activity than the compounds containing simple isatin and 5-bromoisatin. For example, the IC_{50} values of compounds **3h** (R^1 = 2-F, R^2 = H, R^3 = F) and **3i** (R^1 = H, R^2 = H, R^3 = Cl) against the cervical cancer HeLa cell line were 15.14 μM and 10.75 μM respectively, which were better than those of the compounds **3l** (R^1 = 4-CH_3, R^2 = H, R^3 = Br, IC50 = 22.08 μM) and **3m** (R^1 = 4-Cl, R^2 = H, R^3 = Br,

IC50 = 35.61 µ M). Among these, the chlorine substituted compound **3i** (R^1 = H, R^2 = H, R^3= Cl) showed good activity with SK-OV-3, HeLa and DU-145 cell lines listed in table S1. The anti-cancer activities of the compounds **3a–r** with various substitution effects on a phenyl ring demonstrated that the modification of the substituted group R^1 at the phenyl was significant, however, the compounds without any substitution (**3a** and **3r**, R^1 = H) showed very poor activity. It is observed from the above analysis that if the compound contains chlorine atom at R^3 position (**3i** and **3j**) shows significant anti-cancer activity against HeLa cell lines. A similar trend was observed with compound **3i** against SK-OV-3 cell line. The compounds containing fluorine atom at R^1 position (**3d**, **3h** and **3p**) showing moderate activity against HeLa cell line whereas in the case of the compound **3g** the fluorine atom is present at R^3 position does not show good activity.

5. Molecular docking studies

Molecular docking is an important tool to study of binding interactions between selected protein and ligands. *In silico* anti-cancer molecular docking experiments were carried out to explore the binding mode of ligands docked into the active cite of histone deacetylases enzyme (PDB ID: 1VKG) by employing the AutoDock Tools-1.5.6.[34] The observed binding energies were depicted in table S2. In this work we are reporting the binding interactions between the synthesized compounds and 1VKG protein receptor were very strong and showed the lowest binding energy values. The docked compounds (**3a-r**) were well fitted in the binding site of the protein 1VKG and gives different polar and non-polar interactions with amino acid residues. Among all, the compound **3m** exhibited least binding energy -9.18 kcal/mol, there are no hydrogen bonds with the amino acid residues and forms nine hydrophobic interactions (pi and alkyl) with the amino acid residues. Whereas, the compound **3r** showed binding energy -9.18 kcal/mol, forms one hydrogen bond with amino acid residue HIS180 (N–H···O, 2.78 Å) and forms ten hydrophobic interactions with the amino acids. In addition, the compound **3o** exhibited good binding energy -9.16 kcal/mol, forms one hydrogen bond with amino acid residues TYR306 (O–H···N, 2.26 Å). The ligand interaction diagrams of the compounds **3m** and **3r** were presented in figure 3 and figure 4.

Table S2. Docking results of the compounds **3a-r** against 1VKG

Entry	Compound	Binding energy (kcal/mol)	No. of hydrogen bonds	Residues involved in the hydrogen bonding	Hydrogen bond length (Å)
1	**3a**	-8.82	0	-	-
2	**3b**	-8.99	2	TYR306, PHE208	2.37, 3.21
3	**3c**	-8.60	2	TYR306, PHE208	2.35, 3.19
4	**3d**	-8.53	1	HIS180	2.02
5	**3e**	-8.97	2	TYR306, PHE208	2.32, 3.21
6	**3f**	-8.96	0	-	-
7	**3g**	-8.51	1	HIS180	2.09
11	**3h**	-8.49	1	HIS180	2.06
9	**3i**	-8.74	1	HIS180	2.03
10	**3j**	-8.76	2	TYR306, TYR306	2.52, 2.35
11	**3k**	-8.79	1	HIS180	2.13
12	**3l**	-8.99	1	TYR306	3.0
13	**3m**	-9.18	0	-	-
14	**3n**	-9.14	2	HIS180, HIS180	2.25, 2.57
15	**3o**	-9.16	1	TYR306	2.26
16	**3p**	-8.81	2	HIS180, HIS180	2.74, 2.71
17	**3q**	-8.72	2	TYR306, GLY151	2.40, 2.90
18	**3r**	-9.18	1	HIS180	2.78

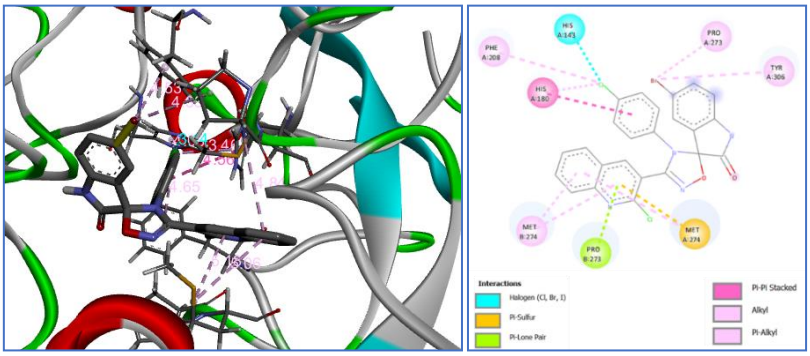

Figure 3. Representing the binding poses and interactions of ligand **3m** and to binding sites of target protein histone deacetylases enzyme (PDB ID: 1VKG protein).

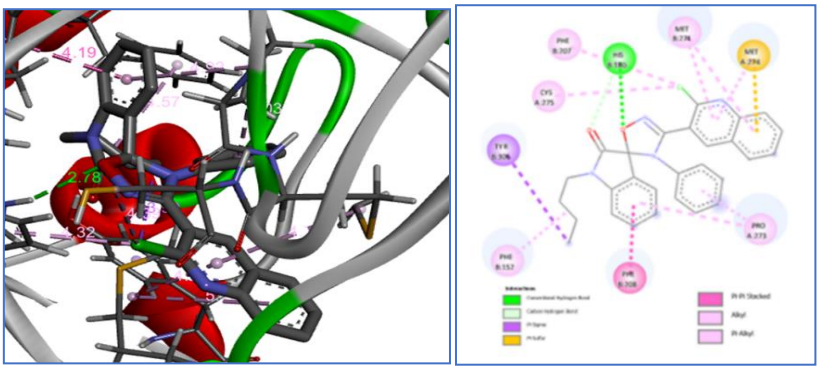

Figure 4. Representing the binding poses and interactions of ligand **3r** and to binding sites of target protein histone deacetylases enzyme (PDB ID: 1VKG protein).

6. ADME Prediction

The *in silico* absorption, distribution, metabolism and excretion (ADME) prediction of the targeted compounds **3a-r** were evaluated by using the online server preADME (https://preadmet.bmdrc.kr/adme/)[35,36] and all the obtained parameters were summarized in table S3. The measurement of ADME makes it easier to identify molecules at the therapeutic dose with a high safety profile. Moreover, the use of *in silico* pharmacokinetic parameters prediction lowers the risk of drug failure during the final stages of a clinical study.

LogP is the measure of octanol/water partition coefficient (lipophilicity). The predicted lipophilicity values are in the ranging from 4.07 to 5.26, and these values revealed that optimal lipophilicity of the compounds. The predicted aqueous solubility (LogS) values for the synthesized compounds varied from -5.98 to -7.48, which indicates their poorly solubility in aqueous media. The results from logarithm of the apparent permeability co-efficient (logPapp) suggests that all the compounds have acceptable Caco-2 permeability. Remarkably, all the synthesized compounds have high human intestinal absorption (HIA: 97.24–98.03%). Blood-brain partition co-efficient (logBB) values of the synthesized compounds are in acceptable range to cross the blood-brain barrier (BBB). The reported drug like properties and *in silico* ADME prediction revealed that the title compounds **3a-r** exhibit adequate pharmacokinetic parameters and can be considered as lead molecules for the development of future pharmacophores.

Table S3. Prediction of ADME properties of the title compounds

Compound	Mol. Wt.	[a]HIA	[b]Caco2	[c]MDCK	[d]Plasma Protein Binding	[e]BBB	[f]Skin Permeability	[g]Rule of five
3a	426.86	97.24	24.05	90.26	100	0.62	-2.75	1
3b	440.88	97.31	24.96	62.33	100	0.48	-2.69	1
3c	444.85	97.25	24.64	30.29	99.96	0.39	-3.05	1
3d	444.85	97.25	24.55	79.79	100	0.61	-2.99	1
3e	461.30	97.52	25.91	56.39	100	0.44	-2.68	1
3f	461.30	97.52	26.79	69.45	100	0.51	-2.68	1
3g	444.85	97.25	24.51	42.16	100	0.39	-3.05	1
3h	462.84	97.26	25.31	34.29	100	0.41	-3.22	1
3i	461.30	97.52	25.63	61.98	100	0.44	-2.68	1
3j	495.74	97.70	29.16	51.57	100	0.57	-2.58	1
3k	505.76	97.66	26.28	0.14	100	0.45	-2.62	2
3l	519.78	97.69	27.56	0.05	99.57	0.54	-2.57	2
3m	540.20	97.78	28.05	0.04	100	0.59	-2.56	2
3n	440.89	97.88	32.87	78.89	100	2.73	-2.58	1
3o	454.91	97.93	34.43	51.95	100	2.03	-2.54	1
3p	458.88	97.89	34.42	18.18	97.83	1.99	-2.87	1
3q	458.88	97.89	34.32	69.56	99.93	2.65	-2.82	1
3r	482.97	98.03	40.29	62.11	96.70	0.96	-2.15	1

[a]Human intestinal absorption, 70-100% good absorption; [b]>90 high permeability; [c]ranging from $3.4x10^{-6}$ to $20.2x10^{-6}$; [d]>90% strongly plasma protein binding; [e]>0.40 CNS active compound; [f]ranging from -6.1 to -0.19; [g]n-violation $\leq$1.

